SCIREA Journal of Electrics, Communication and Automatic Control

http://www.scirea.org/journal/ECAC

October 28, 2016

Volume 1, Issue1, October 2016

Multipulse Heterogeneous Analysis of CA_GTM Adaptive Scheme for Fluctuating Radar Targets

Mohamed B. El_Mashade

Electrical Engineering Dept., Faculty of Engineering, Al Azhar University, Nasr City, Cairo, Egypt.

MohamedElMashade@Gmail.com

Abstract

To mitigate the deleterious effects of clutter and jammer, modern radar have adopted adaptive processing techniques such as CFAR detectors. The aim of these processors is to automatically detect targets in the case where the clutter environment is partially unknown and/or has varying statistical properties maintaining the rate of false alarm at fixed low level. The CA scheme has an optimum detection performance among the mean level CFAR family in the case of homogeneous noise when the neighboring reference cells of sliding window contain the noise data obeying the same PDF and having the same statistical parameters as the data stored in the test cell of sliding window. However, the reference cells are often contaminated by power variations over range, clutter discretes, and other outliers. Additionally, the strength of the clutter also fluctuates with terrain type, elevation, ground cover and the presence of man-made structures. In these situations, the estimating cells may not be representative of the disturbance in the test cell and the CA exhibits strong

degradations both in the detection performance as well as in the CFAR behavior. In the real world, still sub-optimal performance might occur (high false alarm rate and/or low detection probability) as a consequence of heterogeneous clutter, dense target backgrounds, and large discrete and spiky clutter. Therefore, the heterogeneous improvement possibility of this algorithm is of primary concern. This paper is devoted to the analysis of a sophisticated version, which is a combination of CA and GTM, of CFAR schemes collecting data from M-pulses and operating in multitarget environment to detect fluctuating targets of χ^2-distribution with two-degrees of freedom. This version optimizes good features of the well-known CFAR detectors with the goal of enhancing the detection probability and keeping the false alarm rate unchanged. Our numerical results are focused on the important SWI & SWII models because of the prevalence of frequency diversity between noncoherent pulse bursts. In the presence of postdetection integration of M-pulses, it is found that the homogeneous performance of the novel version surpasses that of the fixed-threshold scheme especially for targets obeying SWII model in their fluctuations.

Key words: Adaptive detection, noise and clutter, CA_GTM-CFAR algorithm, postdetection integration, target fluctuation models, multitarget environments.

Introduction

Radars have the objective of performing significant general functions, with all the specific applications falling into one or more of these considerable functions. Depending on the type of radar application, the system might be concerned with estimating the target radar cross section (RCS), measuring and tracking its position or velocity, imaging it, or providing fire control data to direct weapons to the target. The searching function represents the backbone role of any radar system based on which it decides to continue or stop its operations. From this point of view, radar is defined as an instrument that is utilized in observing a natural environment and in detecting physical objects herein. To achieve this goal, it emits electromagnetic waves to illuminate the environment and receives echoes reflected by the objects. In the illuminated environment, numerous objects may introduce reflection and scattering of the transmitted radar signal, causing difficulties in identifying the objects of interest which are termed as targets whilst the interfering echoes are designated as clutter. At

its receiving end, on the other hand, the incoming signal is processed, to see if it is regarded as interference only, or interference plus echoes from a target of interest, before it is displayed to the user. The ability to detect objects at long distances, or in conditions of poor visibility, is the key feature of any radar system. This is of particular importance for aircrafts and ships in order to navigate safely and avoid collisions. Additionally, the radar needs to posses the capability to suppress both clutter and jamming to become near or below the noise level. In this way, the sensitivity of the radar is fully used in signal environments containing unwanted interference. Modern radar systems perform this detection automatically in the signal/data processor. It is achieved by constructing a threshold signal level, on the basis of the current interference, and deciding the presence of a target by comparing the incoming signal level with that threshold. If the signal level exceeds the threshold, then the presence of a target is declared, otherwise no target is proclaimed. In most radar detectors, the threshold is set in order to achieve a required probability of false alarm. However, in most fielded systems, unwanted clutter and interference sources mean that the noise level changes both spatially and temporally. In this case, a changing threshold can be used, where the threshold level is raised and lowered to maintain a constant probability of false alarm. This is known as constant false alarm rate (CFAR) detection. On the other hand, the challenges with automatic detection are prediction of the clutter power, and handling of nonhomogeneous environments. If the statistics of the interference are known a priori, a threshold may be selected to guarantee a specific rate of false alarm. In many cases, the form of the probability density function (PDF) associated with the interference is known, but the parameters of the distribution are either unknown or change temporally or spatially. CFAR strategies are designed to track changes in the interference and to adjust the detection threshold to safeguard the level of false alarm constant [1-5].

Several variants of the CFAR algorithm have been proposed in the radar literature to deal with different problems associated with radar applications. These techniques require linear operations (such as getting the maximum, minimum, or average of a set of values) or nonlinear operations like sorting a set of values and selecting one on a specific position before performing a linear operation. Recently, the cell-averaging- trimmed-mean (CA_TM) CFAR detector optimizes good features of two well-known schemes in the CFAR world depending on the characteristics of clutter and present targets with the goal of increasing the detection performance given that false alarm rate is held unchanged. It is realized by parallel operation of CA- and TM-CFAR procedures [6-9].

Normally, the detection process is performed on the received signal after whatever processing the signal experiences. It may be that a decision is made on the basis of a single transmitted pulse, though this is rare. More often, several pulses are transmitted and the resulting received signal is integrated or processed in some way to improve the signal-to-noise ratio (SNR) compared with the single-pulse case. In any case, to detect the target signal with some reasonable probability and to reject noise, the signal must be larger than the noise. Although there are several techniques of pulse integration, the noncoherent technique is the commonly used one, even though it is not ideally preferred. This is owing to its ease of implementation [10-13].

Realistically, the amplitude of the signal at the receiver input depends on the target radar cross section (RCS) which is a measure of the amount of the electromagnetic energy that a radar target intercepts and scatters back towards the receiver. The nonfluctuating target is one in which the RCS remains constant over the group of samples used for detection. While this is a useful reference point, it is rarely a realistic model of real-world radar targets. Because of the effect of multiple scatterers constructively and destructively interfering with each other, most targets of interest present echo voltages that vary randomly from pulse to pulse, from dwell to dwell, or from scan to scan. In addition, variations in radar-target geometry, target vibration, and radar frequency changes can lead to variations in target RCS, resulting in fluctuating targets. In other words, the target RCS fluctuates due to characteristics of the targets which encompass many scattering elements and the returns from each one of these elements vary. These fluctuations in target RCS are randomly in their nature and must be statistically modeled to facilitate the processor performance evaluation. The Swerling models are the most commonly used in this situation [3,4,8,12].

Our goal in this paper is to analyze the performance of the CA_GTM-CFAR detector in nonideal background conditions when the radar receiver includes a postdetection integrator amongst its contents. Section II is devoted to the description of the processor under consideration along with the formulation of the problem. Section III deals with the processor heterogeneous performance analysis, whilst our simulation results, to compare the homogeneous as well as multitarget performance of the underlined processor with that of other well-known CFAR schemes are displayed in section IV. Finally, our concluded remarks are discussed in section V.

Detector Description and Problem Formulation

Noise is the unwanted energy that interferes with the ability of the receiver to detect the wanted signal. It may enter the receiver through the antenna along with the desired signal or it may be generated within the receiver. The automatic detection of signals (targets) in additive interference (clutter and noise) is not a problem completely solved nowadays. CFAR detection is a set of techniques designed to provide predictable detection and false alarm behavior in realistic interference scenarios. This set of detection strategies is developed according to clutter models and logic used to estimate the unknown clutter parameters. In these detection algorithms, the noise strength around the cell under test (CUT) is estimated and then the threshold level is calculated. The idea of this calculation is to employ a sliding window consisting of $N/2$ reference cells in front of and behind the tested cell, as shown in Fig.(1). The CUT will be denoted by a random variable Y, and the reference cells will be represented by random variables X_i, where $1 \leq i \leq N$. In order to limit error in the adaptive threshold due to the leakage of the target's energy to the neighborhood cells, the two, which are termed as guard, cells directly adjacent to the CUT will not be used in the estimation of the clutter power. Values in the reference cells are used to calculate an estimate of the clutter mean. After estimation, the local threshold value V_T is to be obtained. This is done by multiplying the estimated mean with some scaling factor, commonly termed as the CFAR multiplier, which is derived from a statistical distribution model fitted to the amplitude or power of the clutter. Finally, a decision rule is applied to determine whether a target is present or absent [1].

An efficient CFAR circuit has to fulfill some requirements as: efficient implementation regarding required processing power and production costs, low CFAR loss, accurate fitting of the CFAR threshold to the clutter scenario, the predicted threshold must pass point targets and extended targets, closely spaced targets must not mask each other, and finally the constructed threshold must follow steep rises (or falls) in background clutter amplitude with as little lead (or lag) as possible [11].

The aim of the CFAR algorithm is to maximize the level of detection (P_D) and to keep an acceptable rate of false alarm (P_{FA}) through a variety of signaling environments: homogeneous, multiple targets, and clutter wall. This is achieved through the setting of the detection threshold based on the estimate of the background noise power level and therefore it can automatically adjust it in order to follow the variations in the background noise level. CA

algorithm is the optimal detector, under a condition that the samples of the reference window are independent and identically distributed (IID) and obey exponential distribution. In practice, its performance loss is serious in two cases: when there is a clutter edge, e.g., at the border of land and sea, and if there is an outlier, e.g., a clutter spike, an impulsive interference, or another interfering target This is because of the nonhomogeneity of clutter within a reference window which makes the above assumption invalid. So, the process of CFAR detection cannot be realized and even affect the reliability of test results. Thus, it requires appropriate detection scheme to make the appropriate treatment for the specific circumstances.

Recently, a novel cell-averaging-trimmed-mean (CATM) CFAR scheme has been appeared [7]. It optimizes good features of some well-known CFAR processors depending on the characteristics of clutter and present targets with the goal of improving the detection performance holding the false alarm rate unchanged. It is realized by parallel operation of CA and TM algorithms. These familiar schemes operate simultaneously and independently but with the same scaling factor of the detection threshold "T". They produce own mean clutter power level *Z* using the appropriate CFAR procedure. Next, they calculate own detection thresholds and finally they decide about target presence independently.

Scientifically, it is known that when several detectors are employed simultaneously, as could arise in the weak signal case, a fusion algorithm is used to arrive at a global decision. Based on this rule, the finite decision about target presence is made in fusion center which is composed of an AND logic gate. If both the input single decisions to the fusion center are positive, the global decision of the fusion center is the target presence in the content of the CUT. In each output of other cases, finite decision is negative and the target is absent at the location which corresponds to the cell under test.

After this general insight of the CFAR world, let us go to formulate our interesting problem. In this formulation, it is assumed that a narrowband matched filter is used at the IF section and the radar receiver contains a square-law envelope detector followed by a sampling circuit. The input signal to the receiver is composed of the radar echo signal s(t) and additive zero mean white Gaussian noise n(t), with variance σ^2. The input noise is assumed to be spatially incoherent and uncorrelated with the signal. The output of the band pass IF filter is the signal x(t), which can be written as:

$$x(t) = \begin{cases} x_I(t)\cos(\omega_0 t) + x_Q(t)\sin(\omega_0 t) & in\ trigonometric\ form \\ r(t)\cos(\omega_0 t - \phi(t)) & in\ compact\ form \end{cases} \quad (1)$$

where $\omega_0 = 2\pi f_0$ is the operating frequency, r(t) & φ(t) represent the envelope and the phase of x(t), whilst the subscripts I & Q refer to its in-phase and quadrature components, respectively. The IF filter output is a complex random variable that is composed of either noise alone or noise-plus-target return (sine wave of amplitude A). The quadrature components corresponding to these cases are:

$$\begin{bmatrix} x_I(t) \\ x_Q(t) \end{bmatrix} = \begin{bmatrix} r\cos\phi \\ r\sin\phi \end{bmatrix} = \begin{cases} \begin{bmatrix} n_I(t) \\ n_Q(t) \end{bmatrix} & \textit{in the 1st case} \\ \begin{bmatrix} A+n_I(t) \\ n_Q(t) \end{bmatrix} & \textit{in the 2nd case} \end{cases} \tag{2}$$

A target is detected when r(t) exceeds the threshold value V_T, where the decision hypotheses are:

$$\begin{matrix} s(t)+n(t) \\ n(t) \end{matrix} \quad \begin{matrix} Detection \\ \gtrless \\ False\,Alarm \end{matrix} \quad V_T \tag{3}$$

On the other hand, when the noise subtracts from the signal (while a target is present) to make r(t) smaller than the threshold is known as a miss in the CFAR detection field. Radar designer seeks to maximize the probability of detection for a given probability of false alarm. The noise components $n_I(t)$ and $n_Q(t)$ are uncorrelated zero mean low pass Gaussian processes with equal variances σ^2. Therefore, their joint PDF takes the form:

$$f(n_I, n_Q) = \frac{1}{2\pi\sigma^2} \exp\left(-\frac{n_I^2 + n_Q^2}{2\sigma^2}\right) \tag{4}$$

As a function of r(t) and φ(t), the quadratic noise components can be reformatted as:

$$\begin{bmatrix} n_I(t) \\ n_Q(t) \end{bmatrix} = \begin{bmatrix} r\cos(\phi) - A \\ r\sin(\phi) \end{bmatrix} \tag{5}$$

Taking into account Eq.(4), the above formula gives the joint PDF of the two random variables r(t) and φ(t) which becomes:

$$f(r,\phi) = \frac{r}{2\pi\sigma^2} \exp\left(-\frac{r^2 + A^2}{2\sigma^2}\right) \exp\left(\frac{rA\cos(\phi)}{\sigma^2}\right) U(r) \tag{6}$$

U(.) symbolizes the unit step function. The PDF of r(t) alone can be easily obtained by integrating Eq.(6) over φ which yields:

$$f(r) = \frac{r}{\sigma^2} \exp\left(\frac{r^2 + A^2}{2\sigma^2}\right) I_0\left(\frac{rA}{\sigma^2}\right) U(r) \tag{7}$$

where $I_0(.)$ stands for the zero-order modified Bessel function of the first kind. Conditioned on

the value of the amplitude A, each sample y =$r^2/2$ that originates from a signal at the input of the square-law detector is a random variable with a PDF given by:

$$f_y(y/A) = \frac{1}{\sigma^2} \exp\left(-\frac{y+A^2/2}{\sigma^2}\right) I_0\left(\frac{A\sqrt{2y}}{\sigma^2}\right) U(y) \quad (8)$$

It is well-known that the moment-generating function (MGF) of a random variable is an alternative specification of its probability distribution and it can be used to find all the moments of the distribution also. Owing to the role that the PDF of "Y" can play in our analysis, it is of importance to compute its MGF. The calculation of this statistical parameter can be obtained by transforming Eq.(8) to the λ-domain which gives:

$$\Omega_y(\lambda/s) = \frac{1}{1+\sigma^2\lambda} \exp\left(-\frac{\sigma^2 s\lambda}{1+\sigma^2\lambda}\right) \quad (9)$$

where $s=A^2/2\sigma^2$ denotes the average signal-to-noise ratio (SNR).

Generally, as the frequency diversity among pulse bursts is prevalent in radar detection systems, performance analysis of the adaptive schemes with pulse integration is needed. Although the postdetection technique of pulse integration is not the optimum one, it is the most commonly employed in radar systems due to its ease of implementation. If the returns of M pulses are now noncoherently integrated, the integrator output can be mathematically formulated as:

$$Y \triangleq \sum_{j=1}^{M} y_j \quad (10)$$

Each random variable in that sequence has a MGF similar to that given in Eq.(9). Since the random variables y_j's are assumed to be statistically independent, the integrator output Y has a MGF of the form:

$$\Omega_Y(\lambda/S) = \left(\frac{1}{1+\sigma^2\lambda}\right)^M \exp\left(-\frac{\sigma^2 S\lambda}{1+\sigma^2\lambda}\right) \quad (11)$$

The parameter S is the total, M-pulse, SNR which is M times the single pulse SNR (S = Mxs). The unconditional MGF can be obtained by averaging Eq.(11) over the target fluctuation distribution of S. For the χ^2 family of target models introduced by Swerling, the fluctuating target is characterized by a PDF given by

$$f_S(S/S_a) \triangleq \left(\frac{\kappa}{S_a}\right)^{\kappa} \frac{S^{\kappa-1}}{\Gamma(\kappa)} \exp\left(-\kappa\frac{S}{S_a}\right) U(S) \quad (12)$$

In the above expression, S_a denotes the average of S over the target fluctuation parameter, and κ represents the degree of signal strength fluctuation. In particular, κ =1, M, 2, 2M and ∞ correspond to the SWI, SWII, SWIII, SWIV and SWV, respectively. Therefore, the unconditional MGF of the random variable Y can be easily obtained by calculating the average value of Eq.(11) taking into account the χ^2-distribution of S. Thus,

$$\Omega_Y(\lambda) = \left(\frac{1}{\sigma^2}\right)^M \left(\lambda + \frac{1}{\sigma^2}\right)^{\kappa-M} \left[\left(1 + \frac{S_a}{\kappa}\right)\lambda + \frac{1}{\sigma^2}\right]^{-\kappa} \quad (13)$$

Practically, CFAR algorithm is often implemented after postdetection integration as Fig.(1) displays. The difference between CFAR methods is how the mean estimate is obtained. Because of the effect of multiple scatterers constructively and destructively interfering with each other, most targets of interest present echo voltages that vary randomly from pulse to pulse, from dwell to dwell, or from scan to scan. Therefore, the process of detecting the presence of a target on the basis of the signal voltage is a statistical process, with a probability of detection, P_d, usually less than unity, and some probability of false alarm, $P_{f\,a}$, usually greater than zero. Mathematically, the detection probability has a definition given by:

$$P_d \triangleq \int_0^{\infty} P(Y \geq ZT) \; f_Z(z) \; dz \quad (14)$$

Since Y and Z are statistically independent, letting Θ=Y-ZT leads to

$$\Omega_\Theta(\lambda) = \Omega_Y(\lambda) \; \Omega_Z(-T\lambda) \quad (15)$$

The substitution of Θ in the definition of P_d yields

$$P_d = \int_0^{\infty} f_\Theta(\alpha) \; d\alpha \quad (16)$$

f_Θ (.) represents the PDF of the random variable Θ which can be obtained through the calculation of the Laplace inversion of Eq.(15). Thus, performing this inversion and integrating the resulting form with an allowable change in the order of integration gives

$$P_d = -\sum_{\ell} res\left\{\Omega_Y(\lambda)\frac{\Omega_Z(-T\lambda)}{\lambda}, \lambda_\ell\right\} \quad (17)$$

where the contour of integration lies to the right of all singularities of $\Omega_Y(\lambda)$ in the left half plane, λ_ℓ's (ℓ=1, 2, …) are its poles and res[.] stands for the residue.

Since the MGF of Y is a function of κ and M, we are concerned here with the well-known Swerling models (SWII & SWI). For the SWII target fluctuation model, κ equals M. Thus, the

detection probability can be calculated by substituting Eq.(13), after replacing κ by M, in Eq.(17) which yields:

$$P_d = \left[\sigma^2\left(1+\frac{S_a}{M}\right)\right]^{-M} \lim_{\lambda\to\lambda_2}\left\{\frac{1}{\Gamma(M)}\frac{d^{M-1}}{d\lambda^{M-1}}\left(\frac{\Omega_Z(-T\lambda)}{\lambda}\right)\right\}$$
$$= \left\{\frac{T}{\sigma^2\left(1+\bar{S}\right)}\right\}^M \frac{(-1)^{M-1}}{(M-1)!}\frac{d^{M-1}}{d\lambda^{M-1}}\left[\Psi_Z(\alpha)\right]\Big|_{\alpha=-T\lambda_2=\frac{T}{\sigma^2\left(1+\bar{S}\right)}} \quad (18)$$

$\Psi_Z(.)$, in the above formula, stands for the Laplace transformation of the cumulative distribution function (CDF) of the noise level estimate Z and $\bar{S}$ represents the average per pulse SNR ($\bar{S} = S_a /M$). On the other hand, if the target fluctuates obeying SWI model in its fluctuation, the processor detection performance can be obtained by replacing Eq.(13) into Eq.(17) after substituting κ by 1 as Eq.(12) indicates. The mathematical processing of that substitution leads to:

$$P_d = \frac{T}{\sigma^2(1+S_a)}\left\{\left(\frac{S_a}{1+S_a}\right)^{1-M}\Psi_Z(\alpha)\Big|_{\alpha=\frac{T}{\sigma^2(1+S_a)}} + \frac{\left(1/\sigma^2\right)^{M-1}}{\Gamma(M-1)}\frac{d^{M-2}}{d\lambda^{M-2}}\left[\frac{\Psi_Z(-T\lambda)}{\lambda+\frac{1}{\sigma^2(1+S_a)}}\right]\Bigg|_{\lambda=-\sigma^{-2}}\right\} \quad (19)$$

From Eqs.(18-19), it is evident that the key step in the processor performance evaluation is the determination of the Laplace transformation of the CDF, $\Psi_Z(\lambda)$, of its noise power level Z. For this reason, we focus our attention on deriving it for the underlined detection scheme when it is operated in an environment which is contaminated by target returns other than the target of interest. The motivation of our choosing the nonhomogeneous case for the operating environment is that it is more general than the homogeneous situation and the ideal operation can be easily obtained as a special case by vanishing the returns from outlying targets.

Heterogeneous Processor Performance Evaluation

In practical radar signal detection systems, the problem is to automatically detect a target in a nonstationary noise and clutter background while maintaining a constant probability of false alarm**.** CFAR detection is designated to those techniques that are used to generate adaptive thresholds, and to safeguard the false alarm rate from the environmental changes. Two such techniques will be analyzed in this section, and it is convenient to start with the CA algorithm.

a) Cell-Averaging (CA) Detector

In the CA-CFAR processor, the adaptive threshold is obtained from the arithmetic mean of the reference cells. This CFAR technique is very efficient in case of stationary and homogenous interference. It is often used as basic reference for comparison purposes when investigating other CFAR schemes. The CA detector performs well and its performance approaches that of the Neyman-Pearson detector, as the number of range cells increases to infinity, given that the noise samples obtained from the range cells are independent and identically distributed. Actually, the real environments may include spurious targets and/or clutter edges. The CA processor turns out to perform very poorly in these situations. It suffers from some problems of detection when close targets are observed in a multi-target environment or when clutter conditions changes for adjacent regions in the scan. In other words, its detection performance and false alarm regulation properties may be seriously degraded in nonhomogeneous background; especially if the interference is nonstationary which is often caused by adjacent radar or other radio-electronic devices.

Since both the noise and Rayleigh targets have Gaussian quadrature components, the output of the square-law detector has a PDF of an exponential distribution. In order to analyze this detector performance when the lagging reference sub-window contains radar returns from a heterogeneous background, as in the case of multiple-target situations, the assumption of statistical independence of the reference cells is retained as in homogeneous case. Suppose that reference sub-window contains R_1 cells coming from spurious targets with strength $\sigma^2(1 + I)$, where I symbolizes the interference-to-noise ratio (INR), and $N/2 - R_1$ cells from clear background with power level of σ^2. Then, the estimated total noise power from the lagging reference sub-window can be formulated as:

$$Z_1 \triangleq \frac{1}{N/2}\left\{\sum_{j=1}^{R_1} X_{S_j} + \sum_{\ell=R_1+1}^{N/2} X_{C_\ell}\right\} \tag{20}$$

In the above expression, X_S represents the content of the reference cell that has spurious target return whilst X_C denotes the same thing for the clear background reference sample. Since the elements of each summation are statistically independent, their corresponding MGF's become:

$$\Omega_S(\lambda) = \left(\frac{1}{\sigma^2(1+I)\lambda+1}\right)^{R_1} \quad \& \quad \Omega_C(\lambda) = \left(\frac{1}{\sigma^2\lambda+1}\right)^{N/2-R_1} \tag{21}$$

Taking into account that the two categories of samples are independent, the noise power level estimate posses a mathematical formula for its M-sweeps MGF given by:

$$\Omega_1(\lambda) = \left(\frac{1}{\sigma^2(1+I)\lambda+1}\right)^{MR_1}\left(\frac{1}{\sigma^2\lambda+1}\right)^{M(N/2-R_1)} \tag{22}$$

Similarly, if the leading sub-window has R_2 cells from outlying target returns and $N/2-R_2$ ones from clear background, it has a similar expression of its M-sweeps MGF. Thus,

$$\Omega_2(\lambda) = \left(\frac{1}{\sigma^2(1+I)\lambda+1}\right)^{MR_2}\left(\frac{1}{\sigma^2\lambda+1}\right)^{M(N/2-R_2)} \tag{23}$$

The leading and lagging noise level estimates have MGF's which are given as functions of $\Omega_1(.)$ & $\Omega_2(.)$ through the relation:

$$\Omega_{Z_1} = \Omega_1(\lambda)\Big|_{\lambda=\frac{\lambda}{N/2}} \quad \& \quad \Omega_{Z_2} = \Omega_2(\lambda)\Big|_{\lambda=\frac{\lambda}{N/2}} \tag{24}$$

Finally, the cell-averaging estimates its unknown clutter power level via the addition of the two estimates Z_1 and Z_2. This estimation has an λ-domain representation of the form:

$$Z_{CA} = Z_1 + Z_2 \quad \& \quad \Omega_{Z_{CA}}(\lambda) = \Omega_{Z_1}(\lambda)\ \Omega_{Z_2}(\lambda) \tag{25}$$

Since the λ-domain representation of the CDF of the noise power estimate represents the backbone of the detection probability calculation, it is obvious that it is necessary to accomplish this representation for our analysis to be completed. In terms of the MGF of Z_{CA}, its CDF has a λ-domain representation described by:

$$\Psi_{Z_{CA}}(\lambda) = \frac{1}{\lambda}\ \Omega_{Z_{CA}}(\lambda) \tag{26}$$

b) Generalized Trimmed-Mean (GTM) Detector

The CA procedure is optimum in the sense of minimizing the detectability loss under homogeneous operation [2,3]. However, the real environments may include spurious targets and/or clutter edges. The CA processor turns out to perform very poorly in these situations, and if some resilience against interferers and/or clutter edges is to be gained, alternative techniques, which trade some additional detectability loss under homogeneity for enhanced robustness in heterogeneous environments, must be adopted. The censoring based algorithms, on the other hand, rely on discarding out the highest and eventually the lowest ranked values

in the reference set prior to carrying on the estimate of the noise power level [12,13]. The linearly combined order statistic type of CFAR mechanisms constitutes an efficient and robust power level estimation for exponentially distributed background observations. The more generalized version of the category is the GTM-CFAR scheme. In this class of adaptive algorithms, the noise level estimation is obtained by sorting, in an increasing order, the candidates of the lagging sub-window such that

$$X_{(1)} \le X_{(2)} \le X_{(3)} \le \ldots\ldots\ldots\ldots \le X_{(\ell)} \le \ldots\ldots\ldots\ldots \le X_{(N/2)} \tag{27}$$

Then L_1 from the lower end and L_2 from the upper end are discarded before adding the remaining samples for the noise level to be estimated. Thus,

$$Z_1^{TM} \triangleq \sum_{k=L_1+1}^{N/2-L_2} X_{(k)} \tag{28}$$

In order to attain an unbiased estimate for the unknown noise power, the last sample in the above summation must be weighted in such a way that

$$Z_1^{GTM} \triangleq \sum_{\ell=L_1+1}^{N/2-L_2} X_{(\ell)} + \gamma X_{(N/2-L_2)} \tag{29}$$

"γ" in the above expression is a weighting parameter the value of which depends on the selected CFAR processor, as Table (I) demonstrates. The ordered samples $X_{(\ell)}$'s, ℓ=1, ……, N/2 are neither independent nor identically distributed random variables even though the original samples X_k's are IID random variables. However, if X_i's are exponentially distributed and fulfilled the IID property, they can be transformed to another sequence of independent elements via the mathematical formula:

$$C_j \triangleq X_{(L_1+j)} - X_{(L_1+j-1)} U(j-2) \ , \qquad j=1,2,\ldots\ldots\ldots,N/2-L_2-L_1 \tag{30}$$

TABLE (I) Trimming and weighted parameter values for the well-known CFAR processors

Parameter / Processor	L_1	L_2	γ
CA	**0**	**0**	**0**
OS(K)	**K - 1**	**N/2 - K**	**0**
CCA(K)	**0**	**N/2 - K**	**0**
CML(K)	**0**	**N/2 - K**	**N/2 - K**
TM(T_1, T_2)	**T_1**	**T_2**	**0**

The statistic of GTM processor can be simplified through the definition of another set of independent RV's B_j,s the elements of which are given as a function of the elements of the set C_j's by:

$$B_\ell \triangleq \left(L_t - \ell\right)\ C_\ell \quad , L_t \triangleq N/2 - L_1 - L_2 \quad \& \quad \ell \in [1\,, L_t] \tag{31}$$

In terms of the new RV's B_j's, the GTM noise level estimate is simplified to become:

$$Z_1^{GTM} = \sum_{k=1}^{L_t} B_k \tag{32}$$

Since the random variables B_i's are independent, the MGF of Z_1 is simply the product of the individual MGF's of B_i's. To find the MGF of B_j's, it is convenient to calculate the MGF of C_j's. In terms of the λ-domain representation of the CDF of the ordered statistic $X_{(i)}$'s, the MGF of the random variable C_j's can be easily obtained as [13]:

$$\Omega_{C_j}(\lambda) = \begin{cases} \lambda\ \Psi_{X_{(L_1+1)}}(\lambda) & for\ \ j=1 \\ \dfrac{\Psi_{X_{(L_1+j)}}(\lambda)}{\Psi_{X_{(L_1+j-1)}}(\lambda)} & for\ \ 1 < j \le L_t \end{cases} \tag{33}$$

After obtaining the formula (33), the computation of the MGF of the noise level estimate Z_1 becomes an easy task owing to the independency of its elements. Thus,

$$\Omega_{Z_1}(\lambda) = \prod_{\ell=1}^{L_t} \Omega_{C_j}(\lambda)\Big|_{\lambda = \left(L_t - \ell\right)\lambda} \tag{34}$$

In order to complete the performance analysis of the underlined detector, the λ-domain depiction of CDF of ordered-statistics $X_{(j)}$'s must be calculated. To achieve this goal, we are going to evaluate the CDF of the ℓth ranked sample (out of a total of N/2 samples) when there are R_1 candidates of the lagging reference sub-window contaminated with spurious target returns. This CDF has a mathematical form given by [4]:

$$F_{X_{(\ell)}}^{NH}(y) = \sum_{i=\ell}^{\frac{N}{2}} \sum_{j=Max(0,i-R_1)}^{Min\left(i,\frac{N}{2}-R_1\right)} \binom{\frac{N}{2}-R_1}{j} \binom{R_1}{i-j} \left[1-F_c(y)\right]^{\frac{N}{2}-R_1-j} F_c(y)^j \left[1-F_s(y)\right]^{R_1-i+j} F_s(y)^{i-j} \tag{35}$$

In the above expression, $F_c(.)$ represents the CDF of the cell that contains clear noise only whilst $F_s(.)$ denotes the same thing for the cell that has spurious target return. For M-sweeps, these CDF's have mathematical formulas such that [.]:

$$F_c(y) \triangleq \int_0^y \left(\sigma^2\right)^M \frac{q^{M-1}}{\Gamma(M)} \exp\left(-\frac{q}{\sigma^2}\right) dq$$

$$= 1 - \sum_{m=0}^{M-1} \left(\frac{y}{\sigma^2}\right)^m \frac{1}{\Gamma(m+1)} \exp\left(-\frac{y}{\sigma^2}\right) \tag{36}$$

Similarly,

$$F_s(x) = 1 - \sum_{n=0}^{M-1} \left(\frac{x}{\sigma^2(1+I)}\right)^n \frac{1}{\Gamma(n+1)} \exp\left(-\frac{x}{\sigma^2(1+I)}\right) \tag{37}$$

To calculate the λ-domain representation of Eq. (35), we rewrite it in another simpler form as:

$$F_{X_{(\ell)}}^{NH}(y) = \sum_{i=\ell}^{N/2} \sum_{j=Max(0,i-R_1)}^{Min(i,N/2-R_1)} \binom{N/2-R_1}{j} \binom{R_1}{i-j} \sum_{\alpha=0}^{j} \sum_{\gamma=0}^{i-j} \binom{j}{\alpha} \binom{i-j}{\gamma} (-1)^{\alpha+\gamma}$$
$$\left[\sum_{m=0}^{M-1} \frac{\left(y/\sigma^2\right)^m}{\Gamma(m+1)} \exp\left(-\frac{y}{\sigma^2}\right)\right]^{N/2-R_1+\alpha-j} \left[\sum_{n=0}^{M-1} \frac{\left(y/\sigma^2(1+I)\right)^n}{\Gamma(n+1)} \exp\left(-\frac{y}{\sigma^2(1+I)}\right)\right]^{R_1+\gamma+j-i} \tag{38}$$

The transformation of the above formula into λ-domain results in an analytical expression of the form:

$$\Psi_{X_{(\ell)}}(\lambda) = \sum_{i=\ell}^{N/2} \sum_{j=Max(0,i-R_1)}^{Min(i,N/2-R_1)} \binom{N/2-R_1}{j} \binom{R_1}{i-j} \sum_{\alpha=0}^{j} \sum_{\gamma=0}^{i-j} \binom{j}{\alpha} \binom{i-j}{\gamma} (-1)^{\alpha+\gamma}$$
$$\sum_{\xi_0=0}^{\frac{N}{2}-R_1+\alpha-j} \sum_{\xi_1=0}^{\frac{N}{2}-R_1+\alpha-j} \cdots\cdots\cdots \sum_{\xi_{M-1}=0}^{\frac{N}{2}-R_1+\alpha-j} \frac{\Lambda\left(\frac{N}{2}-R_1+\alpha-j;\xi_0,\xi_1,\ldots\ldots\ldots,\xi_{M-1}\right)}{\prod_{\omega=0}^{M-1}\left[\Gamma(\omega+1)\right]^{\xi_\omega}} \left(\frac{1}{\sigma^2}\right)^{\sum_{\beta=0}^{M-1}\beta\xi_\beta}$$
$$\sum_{\zeta_0=0}^{R_1+\gamma+j-i} \sum_{\zeta_1=0}^{R_1+\gamma+j-i} \cdots\cdots\cdots \sum_{\zeta_{M-1}=0}^{R_1+\gamma+j-i} \frac{\Lambda\left(R_1+\gamma+j-i;\zeta_0,\zeta_1,\ldots\ldots\ldots,\zeta_{M-1}\right)}{\prod_{\nu=0}^{M-1}\left[\Gamma(\nu+1)\right]^{\zeta_\nu}} \left(\frac{1}{\sigma^2(1+I)}\right)^{\sum_{\eta=0}^{M-1}\eta\zeta_\eta}$$
$$\frac{\Gamma\left(\sum_{\beta=0}^{M-1}\beta\xi_\beta + \sum_{\eta=0}^{M-1}\eta\zeta_\eta + 1\right)}{\left[\lambda + \frac{N/2-R_1+\alpha-j}{\sigma^2} + \frac{R_1+\gamma+j-i}{\sigma^2(1+I)}\right]^{\left(\sum_{\beta=0}^{M-1}\beta\xi_\beta + \sum_{\eta=0}^{M-1}\eta\zeta_\eta + 1\right)}} \tag{39}$$

Where

$$\Lambda\left(K;\theta_0,\theta_1,\ldots\ldots\ldots\ldots,\theta_{M-1}\right) \triangleq \begin{cases} \dfrac{\Gamma(K+1)}{\prod_{\varepsilon=0}^{M-1}\Gamma(\theta_\varepsilon+1)} & \text{for} \quad \sum_{\rho=0}^{M-1}\theta_\rho = K \\ 0 & \text{for} \quad \sum_{\rho=0}^{M-1}\theta_\rho \neq K \end{cases} \tag{40}$$

Similarly, if the leading window possesses R_2 outlying target returns among its contents and

$N/2\text{-}R_1$ cells containing clear background, we can follow the same steps to obtain the λ-domain representation of the CDF of its noise power level simply by replacing L_1, L_2, L_t, and R_1 by Q_1, Q_2, Q_t, and R_2, respectively, where Q_1 represents the discarded number of samples from the lower end, Q_2 symbolizes the trimmed number of samples from the upper end, and $Q_t=N/2-Q_1-Q_2$ denotes the remaining number of samples which are summed to estimate the unknown noise power level Z_2 of the leading sub-window. The final noise level is obtained by adding the two noise power level Z_1 & Z_2. Thus,

$$Z_{GTM} = \sum_{\ell=1}^{2} Z_{\ell} \quad \& \quad \Psi_{Z_{GTM}}(\lambda) = \lambda \prod_{\ell=1}^{2} \Psi_{Z_{\ell}}(\lambda) \tag{41}$$

Once the λ-domain representation of the ℓth ordered sample $X_{(\ell)}$ is obtained, the MGF of the noise power level estimate Z_{GTM}, which is the backbone of the processor performance evaluation, can be easily computed, as Eq.(34) demonstrates. Hence, the GTM-CFAR scheme is ready to be combined with the CA-CFAR algorithm to develop CA_GTM-CFAR detector.

c) Cell-Averaging_Generalized Trimmed-Mean (CA_GTM) Detector

The CA_GTM-CFAR processor is designed to exploit the advantages of both CA and GTM detection schemes in order to reach the highest performance in homogeneous as well as heterogeneous background environments in simultaneous with keeping the pre-assigned rate of false alarm constant. It is realized by parallel operation of two types of CFAR schemes: CA- and GTM as Fig.(1) demonstrates. In this novel version of CFAR techniques, CA and GTM schemes process their operations simultaneously and independently in such a way that the thresholding's constant "T" is common for achieving their own detection threshold against which the content of CUT is compared to independently decide the presence or absence of the searching target. The final decision about target presence is made in fusion center which is composed of an "AND" gate circuit. If both the input single decisions in the fusion center are positive, the final decision of the fusion center is presence of the target in the tested sample. Otherwise, the fusion center's decision is negative and target is not at the location which corresponds to the cell under test [14].

Owing to the independency of the single decisions about target presence of CA and GTM candidates of the CA_GTM resulting detector, the global false alarm and detection probabilities can be mathematically formulated as:

$$P_{fa}^{CA\_GTM} = P_{fa}^{CA} \; P_{fa}^{GTM} \quad \& \quad P_{d}^{CA\_GTM} = P_{d}^{CA} \; P_{d}^{GTM} \tag{42}$$

In the above expression, P_n^m denotes the P_n probability for the processor m; where n can represent either false alarm or detection and m symbolizes CA, GTM, or CA_GTM. Since each one of the right hand side of Eq.(42) was previously calculated, the performance of the CA_GTM novel model of CFAR schemes is completely analyzed. Our scope in the next section is to give the reader some numerical examples to take an idea about the new contribution of the novel fashion of adaptive detectors to the world of CFAR processing algorithms.

Performance Evaluation Results

In this section, it is convenient to evaluate and compare, through numerical methods, the performance of the new version of CFAR schemes with that of the well-known detectors in the CFAR field. To see to what extent the novel processor improves the performance of the existing detectors, it is obvious to compare its features with those of the most familiar schemes in the CFAR world. For the purpose of comparison, P_{fa} has the value of 10^{-6} and the size of the reference window N is taken as 24.

Now, we will go to numerically analyze the detection performance of the underlined processors in order to distinguish which one has the highest behavior against the contamination of the background environment. Our presentation results are categorized according to the operating conditions. Firstly, we discuss the detection characteristics of the tested schemes in the case where the functional environment is ideal; i.e. free of any abnormalities except the normal clutter which is homogeneously distributed among the reference samples. The processor homogeneous performance is evaluated in terms of the false alarm and detection probabilities. The numerical example provides some insight into the influence of the various variables on the detector's performance, and therefore assists in the design of proper procedures for determination of the optimum values for its parameters. Owing to the importance of the SWII target fluctuation model in practical applications, Fig.(2) depicts the detection probability as a function of the strength of the primary target return taking into account that the radar receiver collects data from two consecutive pulses (M=2) and the target of interest fluctuates following SWII model in its fluctuation. To see to what extent the noncoherent integration can enhance the adaptive detection performance, the

monopulse behavior of the underlined processors is also incorporated amongst the curves of the considered plot. In our displayed results, we will represent each CFAR scheme with the statistical role used in estimating the obscure noise level from its reference sub-windows. This figure encompasses a set of detectors includes: the conventional CA; GTM(1, 12, 0), the well-known OS; GTM(10, 10, 0), the familiar TM; GTM(3, 10, 0), the new version CA_OS; CA_GTM(10, 10, 0), the novel model CA_GTM; CA_GTM(3, 10, 0), and the optimum; fixed-threshold. The presented algorithms are designated in accordance with Table I. The examination of the groups of curves of Fig.(2) demonstrates that the novel version CA_GTM(3, 10, 0) has the nearest performance to the optimum detector for single sweep case, the conventional OS(10) scheme gives the farthest detection behavior, whilst the other tested processors present a detection reaction in between. The shown results illustrate that the two new models give detection performance which is surpassed that of the CA scheme; the king of homogeneous situation and the novel model of trimmed-mean with excision of two cells from the upper end and two ones from the lower end has higher performance than that of order-statistic with ranked parameter of 10. The fixed-threshold detector has the top performance as predicted. All these observations are associated with monopulse case; i.e. without noncoherent integration. When the radar receiver includes a video integrator next to the square-law device, the novel model CA_GTM(3, 10, 0) outweighs the Neyman-Pearson detector in its homogeneous performance to become the adaptive processor that has the highest detection reaction against the background clutter. The other schemes maintain their locations as in the situation of single sweep. In other words, the sorting of the tested algorithms remains as it is in the absence of noncoherent integration except that the novel version CA_GTM(3, 10, 0) and fixed-threshold detector exchange their positions in such a way that the novel model exceeds the optimum processor which reserves the second position instead of the first one. This category of classification is from the detection performance point of view and for two integrated pulses (M=2). Fig.(3) illustrates the same detection characteristics, as Fig.(2), of the underlined schemes when the primary target obeying in its fluctuation SWI model. In this situation of operating conditions, the new versions present the same behavior as the CA technique which is lower than that of the optimum detector. The standard OS(10) procedure still exhibits the worst, relative to other processors considered here, performance for postdetection integration of two pulses given that its operation lies in an ideal environment.

Let us now add more pulses to the CFAR circuit to see to what extent the processor performance improves with increasing the number of integrated pulses. Fig.(4) shows the same thing, as Fig.(2), for the tested processors given that their processing data are based on integration of three successive pulses (M=3) and the operating environment is still free of any abnormalities. The target under test fluctuates in accordance with SWII model. By comparing the exhibited results of this family of curves with their corresponding ones of Fig.(2), it is illustrated that they behave the same behavior as those of Fig.(2) with an increasing rate of change. There is also an additional performance improvement, relative to the case of two integrated pulses, of each processor and the sequence of distinguishing rests as it is in Fig.(2). The novel version CA_GTM(3, 10, 0) performance exceeds that of the optimum detector and the difference between them becomes obvious. The standard GTM(10, 10, 0) resolves its position where it has the lowest detection performance in comparison with the other tested schemes. For the same circumstances, what will happen if the tested target obeys SWI model in its fluctuation?. Fig.(5) answer this question by plotting detection probability against SNR for the selected CFAR algorithms along with the fixed-threshold scheme when the radar receiver integrates three consecutive sweeps for its processing data. A big insight on the variation of the curves of this graph reveals that they follow the same manner in their variation as their corresponding ones of Fig.(3) with some ameliorations. The optimum processor maintains its location as one that has the top detection characteristics, whilst the new versions exhibit the same detection reaction as the conventional CA procedure.

Since increasing M enhances the processor detection performance, Fig.(6) repeats the same thing as Figs.(2 & 4) for M=4 to obtain more and more improvement in the detection reaction of the under examination schemes in face of background clutter. The same comments can be observed about the behavior of the group of curves of this scene with the indication that the distinction between the novel version and optimum detector becomes evident in such a way that the performance of the novel model of adaptive threshold techniques is preferable than that of fixed-threshold scheme. Fig.(7) iterates the similar object as Figs.(3 & 5) for SWI fluctuation model of the target of interest in the situation where the CFAR circuit has a reference window the content of elements of which is a result of integration of four successive pulses. By examining the curves of the current graph, it is noted that there is no new in their behavior, in comparison with those of the previous indicated figures, except that they possess some additional gain to proceed towards regions of lower SNR.

Generally, the outlined results demonstrate that the technique of noncoherent integration of M consecutive sweeps plays an important part in enhancing the processor detection performance and the rate of improvement attains its maximum at M=2. For M>2, the rate of enhancement decreases as M increases. Additionally, for SWII fluctuating targets, some derived model of adaptive schemes surpass the fixed-threshold algorithm from the detection performance point of view. In other words, these modified versions occupy the position of Neyman-Pearson detector to become the ideal ones against which other detection techniques can be compared. When the tested target fluctuates in accordance with SWI model, the fixed-threshold rests the optimum one which is taken as a reference of comparison in any detection problem.

As a measure of the ability of a CFAR processor to detect fluctuating radar targets, let us go to calculate the required SNR to achieve a pre-assigned level of detection for the tested schemes when their operation lies in a homogeneous environment. Figs.(8 & 9) are concerned with the presentation of the necessary signal strength as a function of the needed probability of detection for the underlined detection algorithms operated without (M=1) and with (M>1) noncoherent integration of M successive pulses. Fig.(8) contains the standard processors along with the new version CA_OS whilst Fig.(9) depicts the same thing for the conventional CFAR procedures including the novel model CA_GTM for M=1, 2, and 4, given that the primary target obeys SWII model in its fluctuation. The displayed results of the first figure in this category of curves show that the fixed-threshold detector is the optimum one that requires the minimum SNR to satisfy the needed detection level and the new version CA_GTM(10, 10, 0) comes next, the standard CA reserves the third position whilst the traditional OS has the last location in the queue. As M increases, lower signal strength is demanded to realize a specified level of detection which means that noncoherent integration enhances the processor detection performance. The rate of enhancement decreases as M increases, as the shown results demonstrate. The results shown in Fig.(9), on the other hand, reveal the superiority of the novel version CA_GTM(3, 10, 0) in achieving the required probability of detection with least SNR on the condition that the radar receiver contains a noncoherent integrator amongst its fundamental components. As we have previously noted in the discussion of the detection characteristics of the tested detectors, the superiority of the novel version than the Neyman-Pearson detector becomes more evident as M increases, which is very clear from the results of Fig.(9).

The contaminated environments are frequently encountered in practical applications. The multiple target operation of radar systems represents one of these fundamental contaminations. In this situation, the presence of interferer's returns among the contents of the reference window constitutes the major source of performance impairment of CFAR algorithms. To visualize the influence of multitarget operation on the CFAR processor performance, we repeat all the aforementioned figures in the case where the background environment comprises some spurious targets besides the target of interest taking into account that the primary as well as the secondary outlying targets fluctuates following χ^2-distribution with two-degrees of freedom (SWII & SWI models). Fig.(10) depicts the detection performance of the considered algorithms when they operate in an environment that contains two, one in each sub-window, interfering targets along with the searched one and all of them fluctuate in accordance with SWII model. The candidates of this figure are parametric in the specified CFAR processor and are drawn in the absence (M=1) as well as in the presence of noncoherent integration of two pulses (M=2). As a reference of comparison, the performance of the optimum detector is incorporated among the curves of this family to see to what extent the processor performance can approach that of the fixed-threshold scheme. The visual inspection of the variation of the elements of this figure illustrates that the CA scheme has the worst performance whilst the trimmed-mean possesses the highest performance and the rest models have performance lies in between. Additionally, the new versions enhance the multitarget performance of the CA procedure, where the novel model CA_GTM(3, 10, 0) gives higher performance than the CA_GTM(10, 10, 0) model. However, the multiple-target performance of the combination of CA and GTM algorithms remains modest, where the level of improvement is insufficient for CA to behave like OS or TM scheme. Fig.(11) iterates the same thing for the indicated detectors when the targets following SWI model in their fluctuation. The set of curves of this figure varies in the same sequence as the corresponding ones in the previous figure with minor degradation in their detection performance. Figs.(12 & 13) repeat the same detection characteristics as Figs.(10 & 11) for M=3. It is noted that there is no new in the variation of the curves of these plots except that there is some gain in comparison with their situation in the case of M=2. The last category of curves in these groups of multitarget detection characteristics includes Figs.(14 & 15). These plots regenerate the same family of curves as the previous ones in the case of noncoherent integration of four consecutive sweeps in order to enhance the processor performance more and more. Each CFAR scheme reserves its position which is unchanged with noncoherent integration. The

benefit of pulse integration is to improve the processor performance without any changes in the ranks of the considered schemes with the fixed-threshold detector occupying the top position.

Finally, we are going to evaluate the needed SNR to satisfy a given level of detection in the presence of two (R_1=R_2=1) fluctuating interfering targets along with the target under test when these targets follow SWII model in their fluctuation. The results of this category of curves are summarized in Figs.(16 & 17). The first plot is concerned with the standard CFAR schemes along with the new version which is CA_GTM(10, 10, 0) whilst the second one is devoted to the same traditional detectors besides the novel model CA_GTM(3, 10, 0) and the results of the optimum processor are incorporated with the two figures for the purpose of comparison. The displayed results of Fig.(16) illustrate that the conventional CA scheme is unable to satisfy a detection level which is higher than a specified value. The new version CA_OS(10) is also incapable to fulfill a desired level of detection beyond a particular value which is higher than that of the conventional CA algorithm. The well-known OS mechanism, on the other hand, is capable to follow any required level of detection where the number of outlying target returns lies within its allowable range [4]. This detector gives a required SNR versus a pre-assigned level of detection which is the nearest one to that given by the optimum algorithm. As it is shown from the curves of the current figure, the noncoherent integration enhances the performance of the signal detection where lower signal strength is needed to attain a given level of detection as long as the number of integrated pulses increases. Fig.(17) regenerates the same characteristics as the previous figure for the novel model CA_TM(2, 2). The exhibited family of curves illustrates that the improvement in the behavior of the traditional CA detector is higher than that obtained by combining it with the OS scheme. This is obvious through the distance between the curve representing the CA and that denoting the CA_TM(2, 2) for each number of integrated pulses. The normal TM(2, 2) detector is able to fulfill whatever level of detection because the number of extraneous target returns is less than the number of samples which is excised from the upper end of each sub-window. This processor possesses a needed SNR variation against required level of detection which is the nearest one to that obtained by Neyman-Pearson scheme.

Conclusions

This paper is concerned with fluctuating target detection under homogeneous as well as heterogeneous clutter background using analytical evaluation processing with the aim of improving the detection probability in such a way that it surpasses that of CA and fixed-threshold schemes when the radar receiver collects data from M-successive pulses to achieve its detection purposes. It is assumed that the considered targets, original and spurious, are fluctuating in accordance with χ^2-distribution of two-degrees of freedom (SWI & SWII models), whilst the clutter has exponential distribution. Here, we put forward combine the advantages of different CFAR techniques to get better detection performance. To benefit the distinguishable homogeneous detection performance of CA algorithm and the recognizable heterogeneous detection performance of GTM processor, we incorporate the two techniques to develop the novel version CA_GTM. We have given a detailed derivation of the detection performance of the new model of CFAR procedures in multitarget situations when this model is supplemented by a video integrator. This type of adaptive radar detectors was found to give noncoherent detection performance which surpasses that of the fixed-threshold strategy when the background environment is homogeneous. In multiple-target environments, it possesses a detection performance which is higher than that of the CA mechanism but still insufficient to reply any required level of detection. The numerical results provide an important insight into the effect of the system's parameters on its performance. These results will be useful for designing the new version of CFAR techniques with noncoherent integration because of the prevalence of frequency diversity between noncoherent pulse bursts in real radar systems.

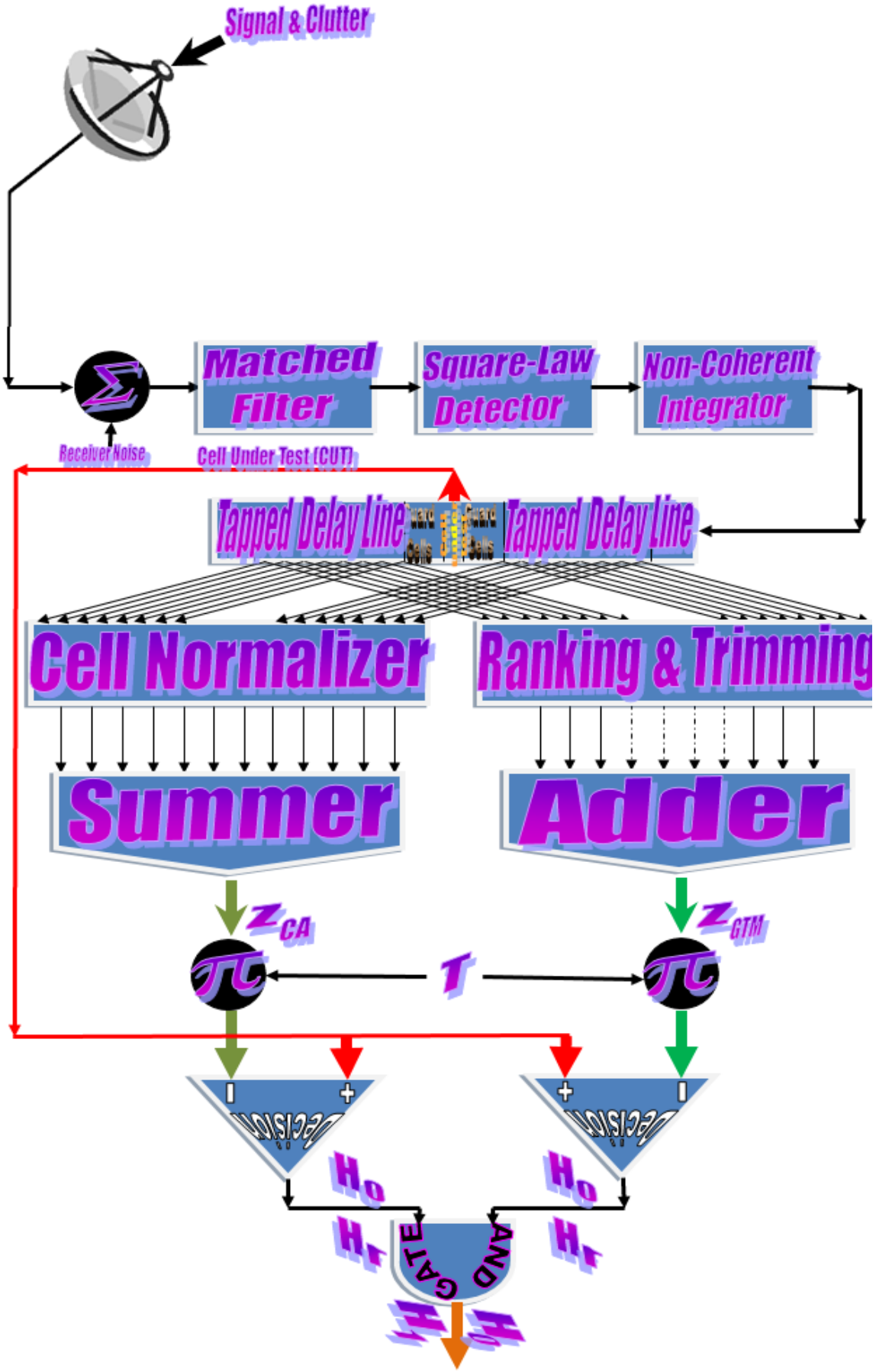

Fig.(1) Architecture of CA_GTM adaptive threshold scheme

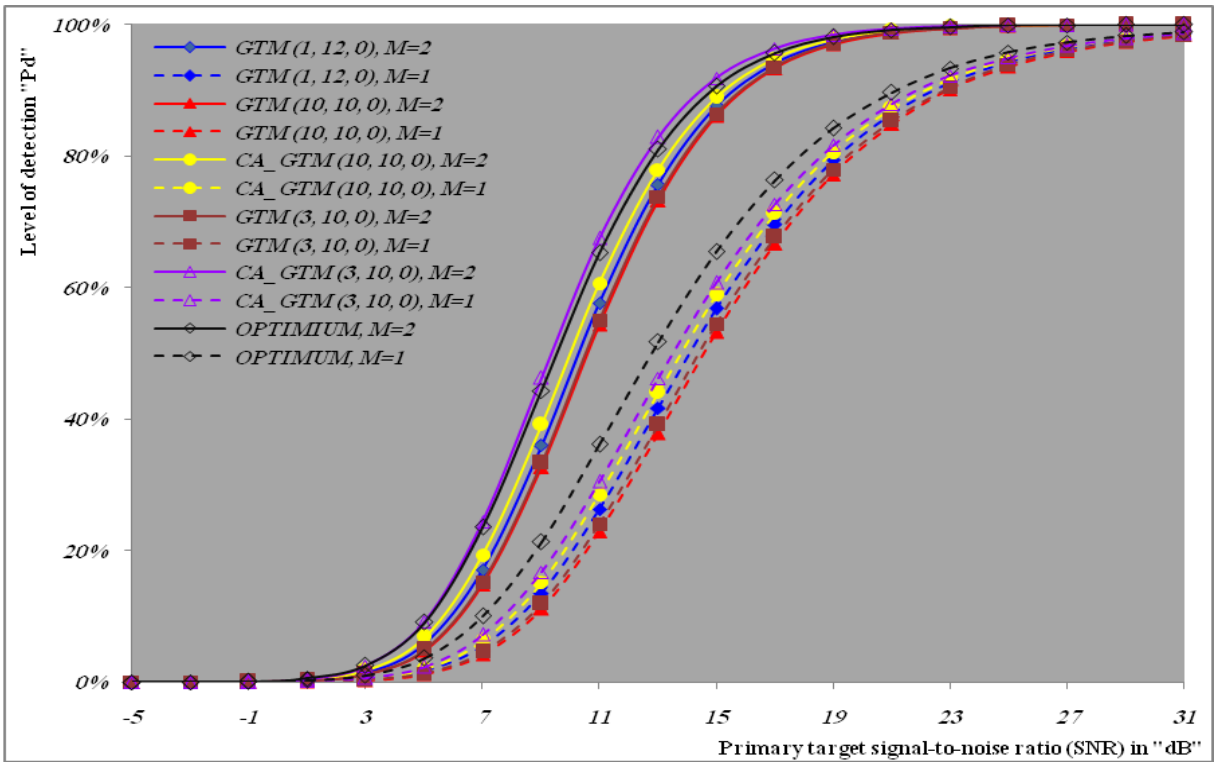

Fig.(2) Multipulse homogeneous detection performance of GTM family of CFAR detectors for SWII target fluctuation model when N=24, M=2, and $P_{fa}=10^{-6}$.

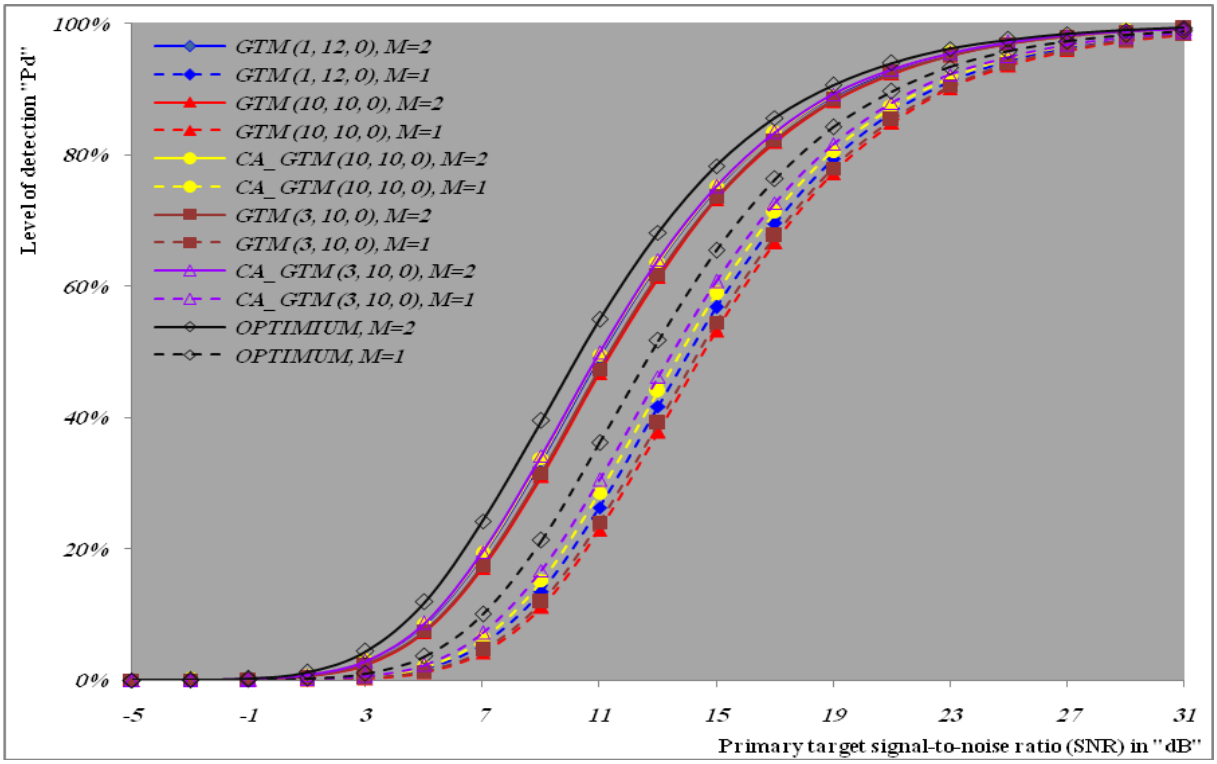

Fig.(3) Multipulse homogeneous detection performance of GTM family of CFAR detectors for SWI target fluctuation model when N=24, M=2, and Pfa=10-6.

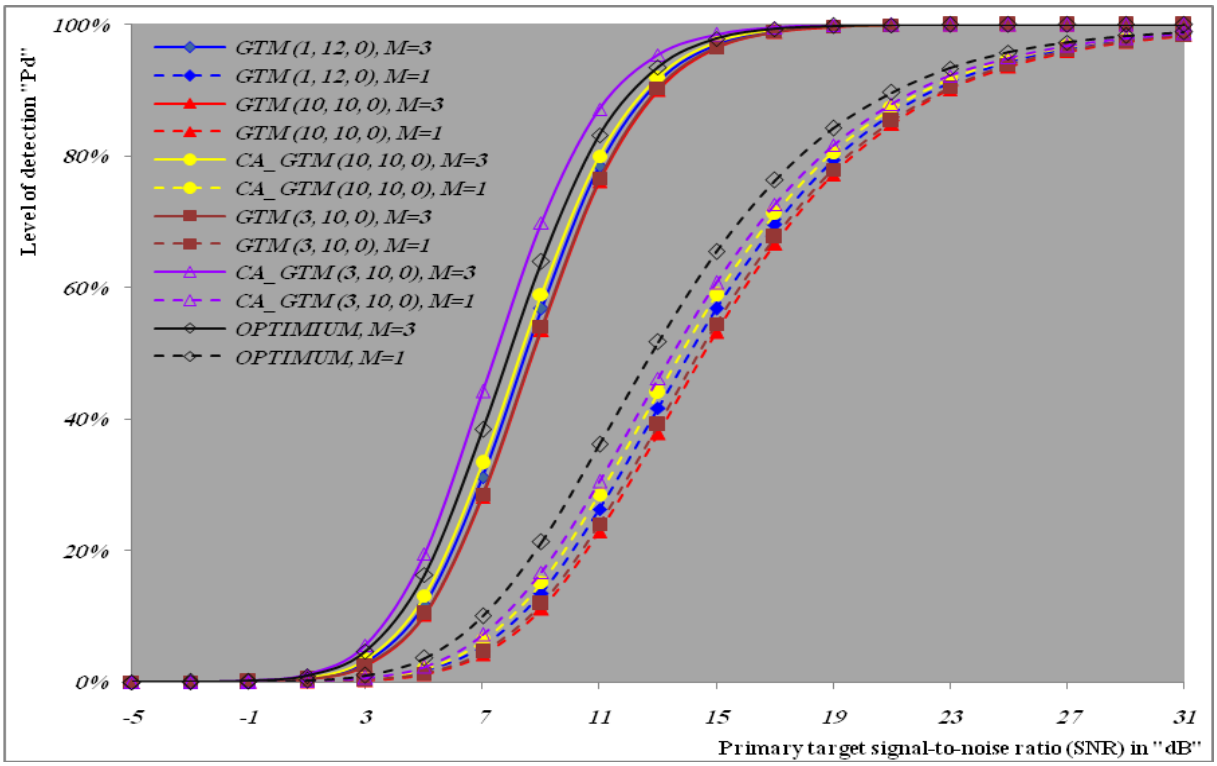

Fig.(4) Multipulse homogeneous detection performance of GTM family of CFAR detectors for SWII target fluctuation model when N=24, M=3, and Pfa=10-6.

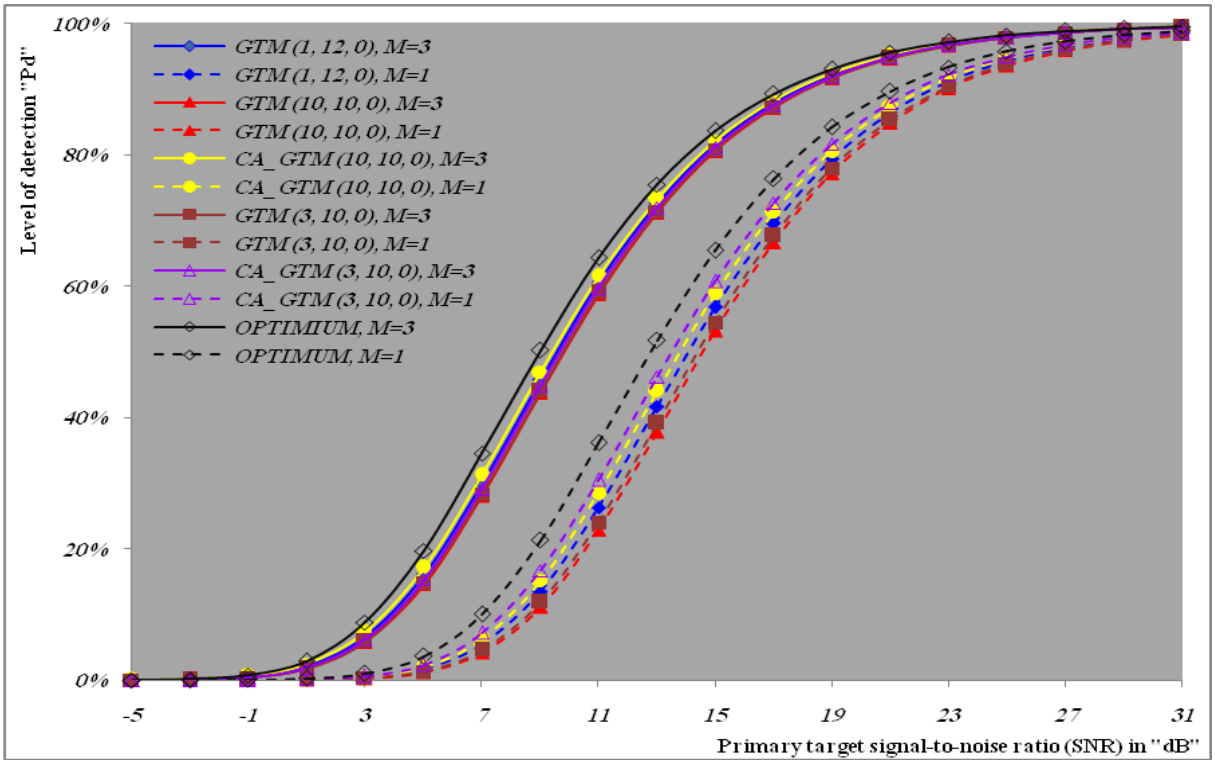

Fig.(5) Multipulse homogeneous detection performance of GTM family of CFAR detectors for SWI target fluctuation model when N=24, M=3, and Pfa=10-6.

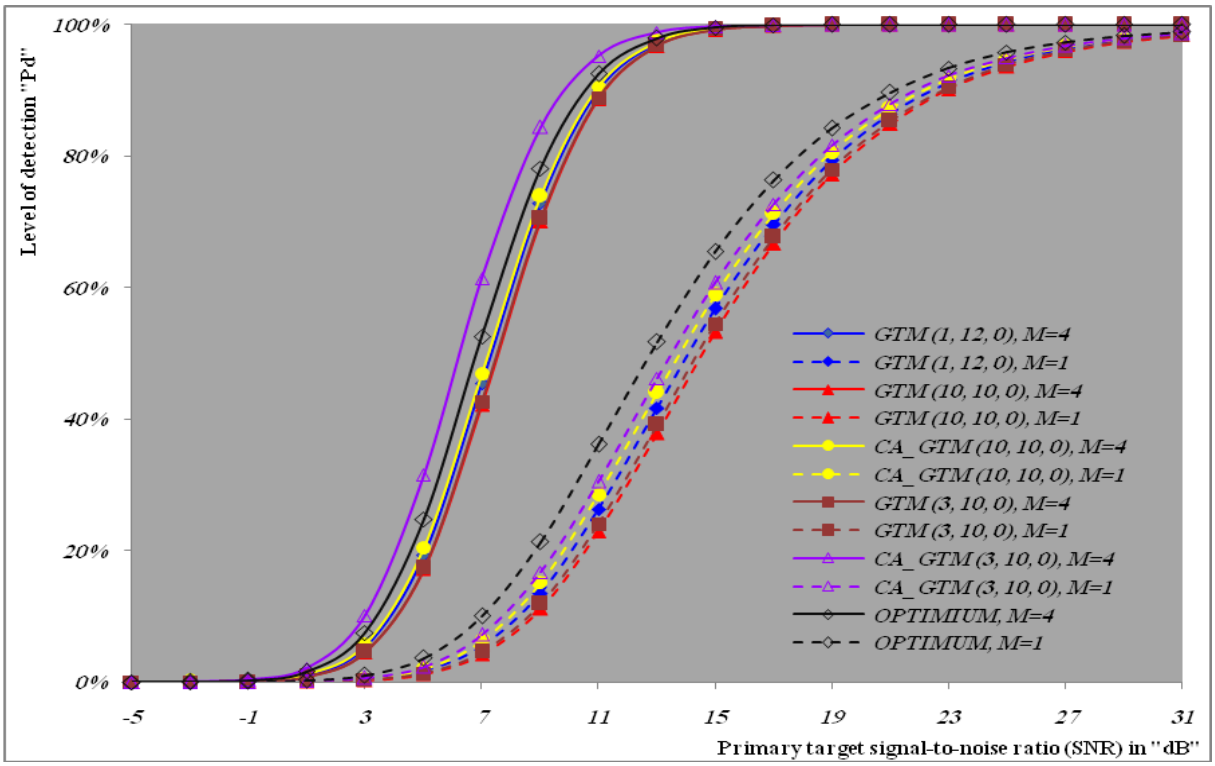

Fig.(6) Multipulse homogeneous detection performance of GTM family of CFAR detectors for SWII target fluctuation model when N=24, M=4, and Pfa=10-6.

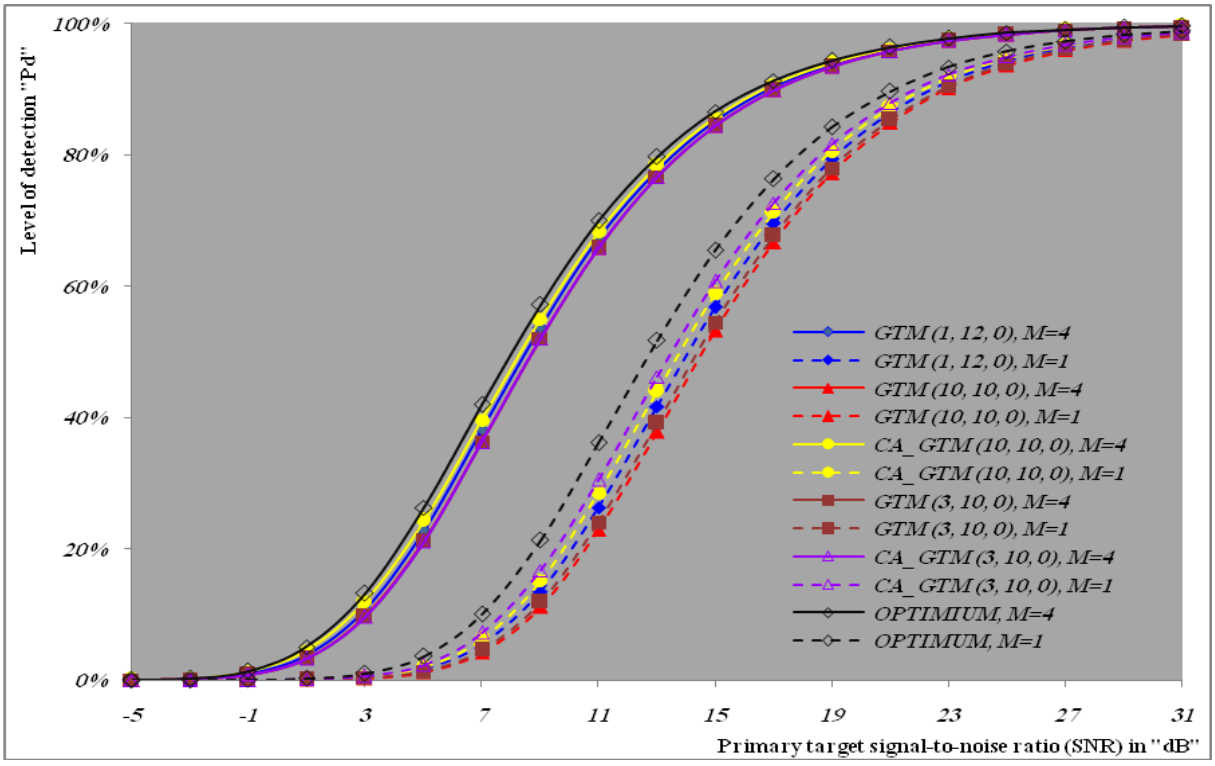

Fig.(7) Multipulse homogeneous detection performance of GTM family of CFAR detectors for SWI target fluctuation model when N=24, M=4, and Pfa=10-6.

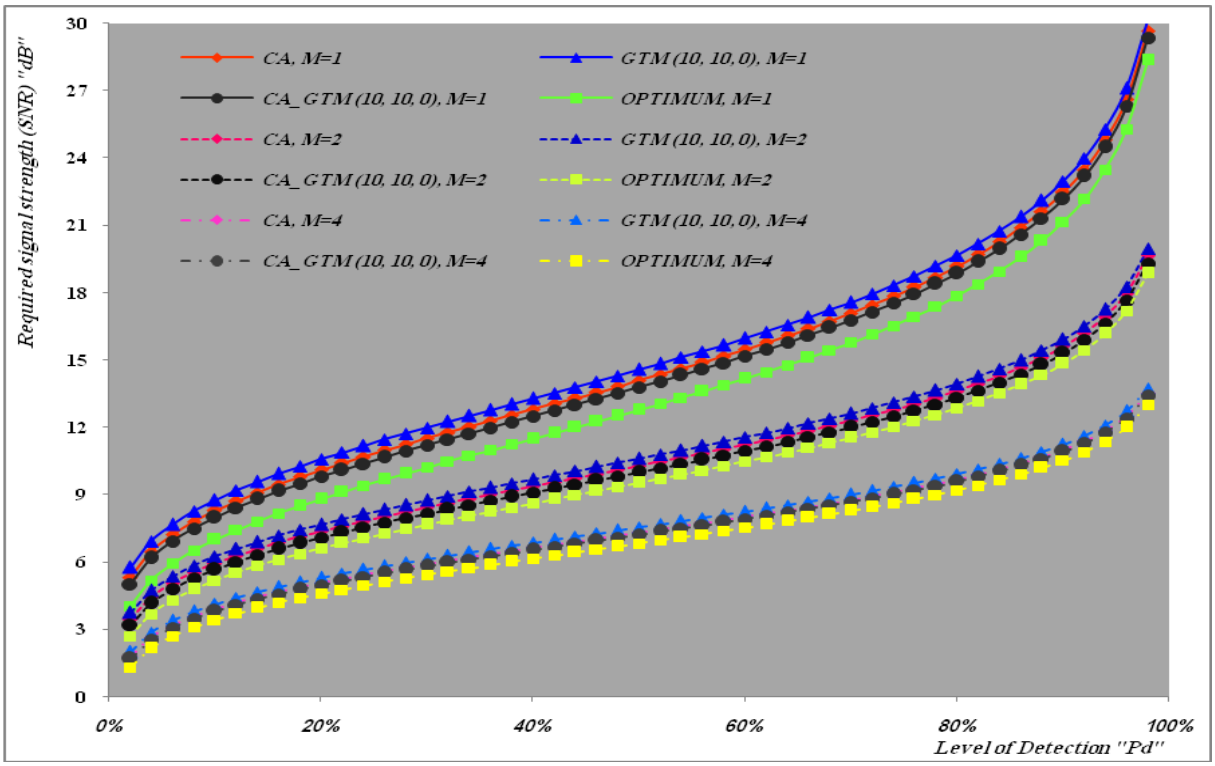

Fig.(8) Homogeneous multipulse required SNR to achieve a given level of detection of OS as well as the developed version of adaptive schemes for SWII target fluctuation model when N=24, and Pfa=10-6

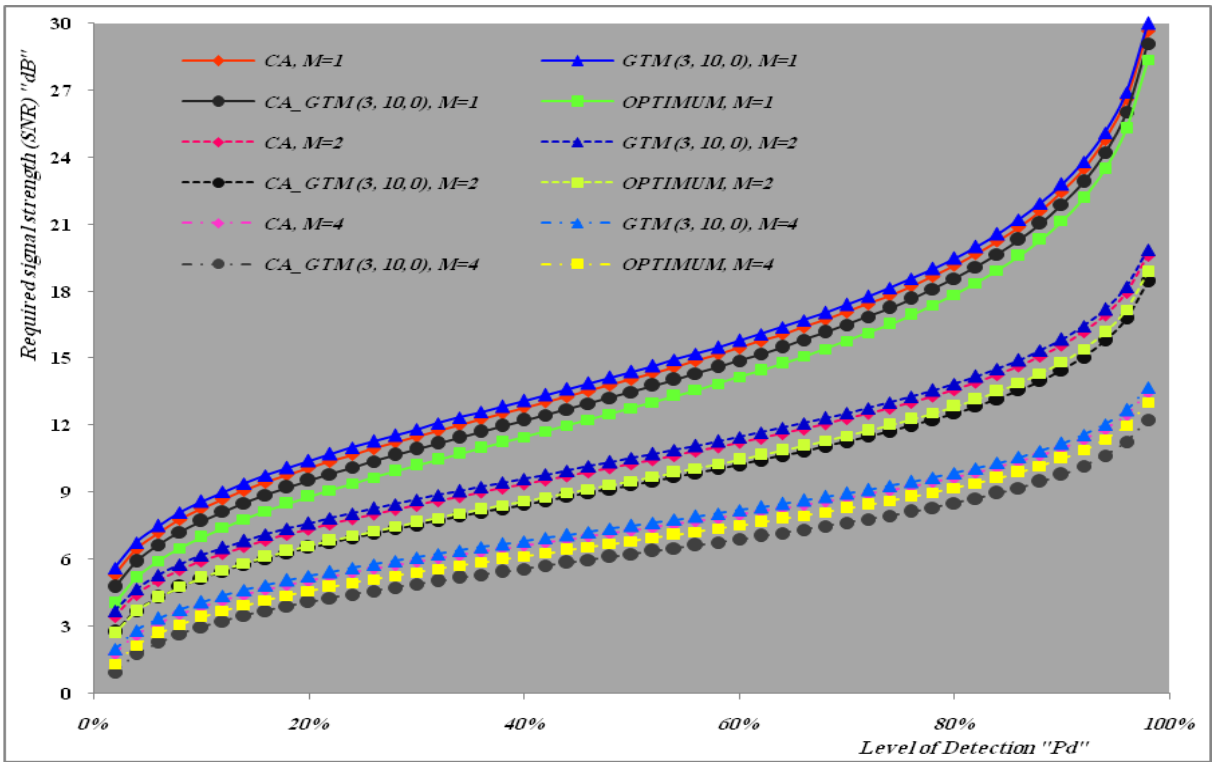

Fig.(9) Homogeneous multipulse required SNR to achieve a given level of detection of TM as well as the developed version of adaptive schemes for SWII target fluctuation model when N=24, and Pfa=10-6

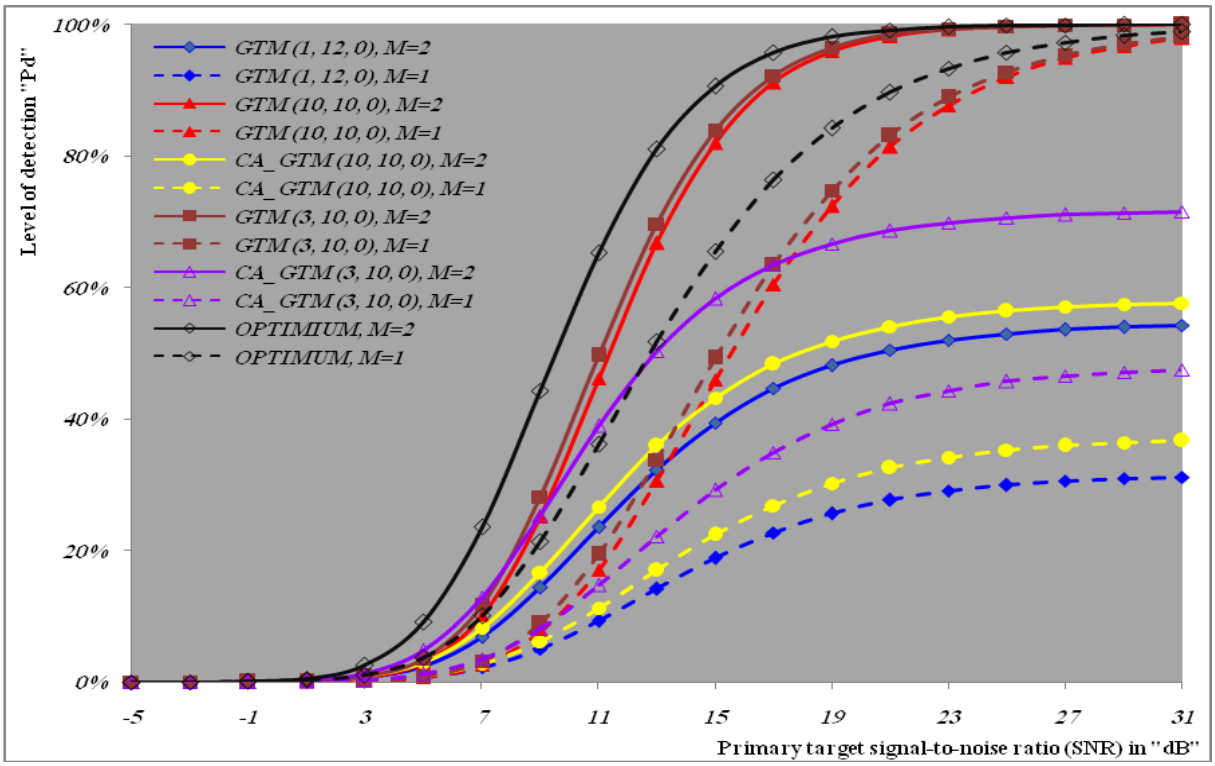

Fig.(10) Multipulse multitarget detection performance of GTM family of CFAR processors for SWII target fluctuation model when N=24, M=2, R1=R2=1, and Pfa=10-6

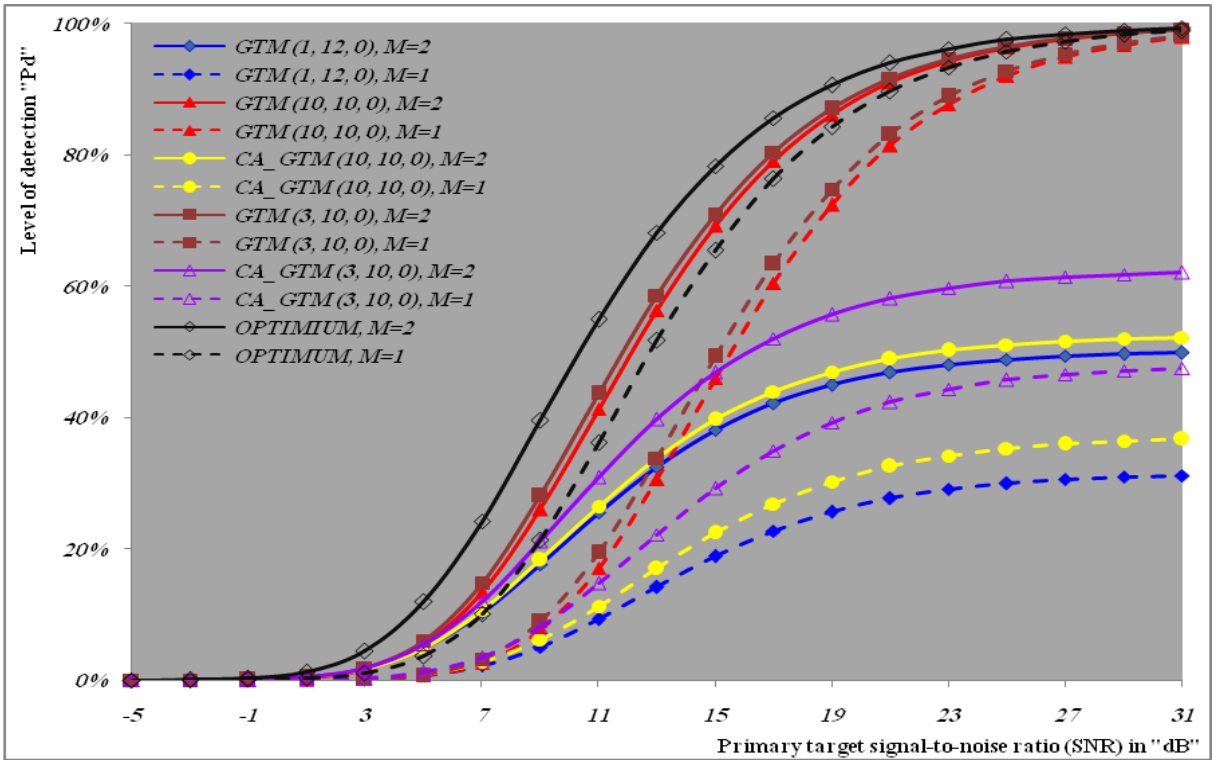

Fig.(11) Multipulse multitarget detection performance of GTM family of CFAR processors for SWI target fluctuation model when N=24, M=2, R1=R2=1, and Pfa=10-6

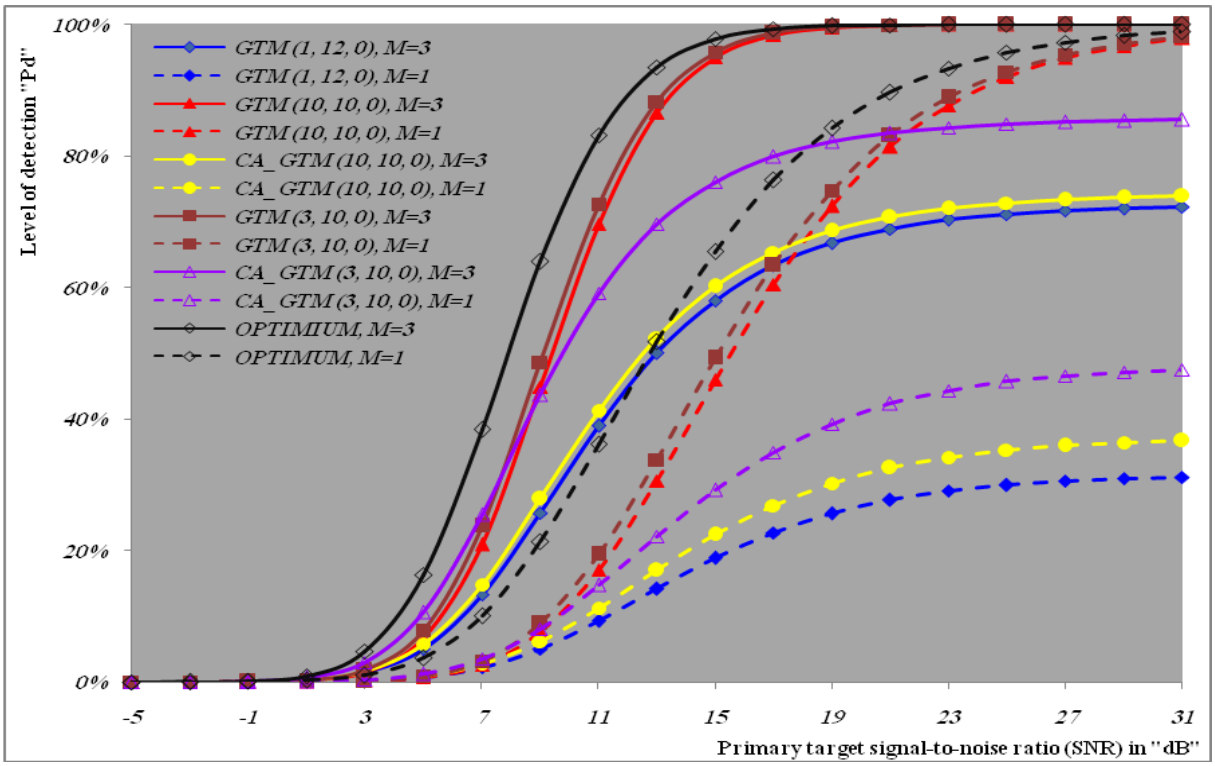

Fig.(12) Multipulse multitarget detection performance of GTM family of CFAR processors for SWII target fluctuation model when N=24, M=3, R1=R2=1, and Pfa=10-6

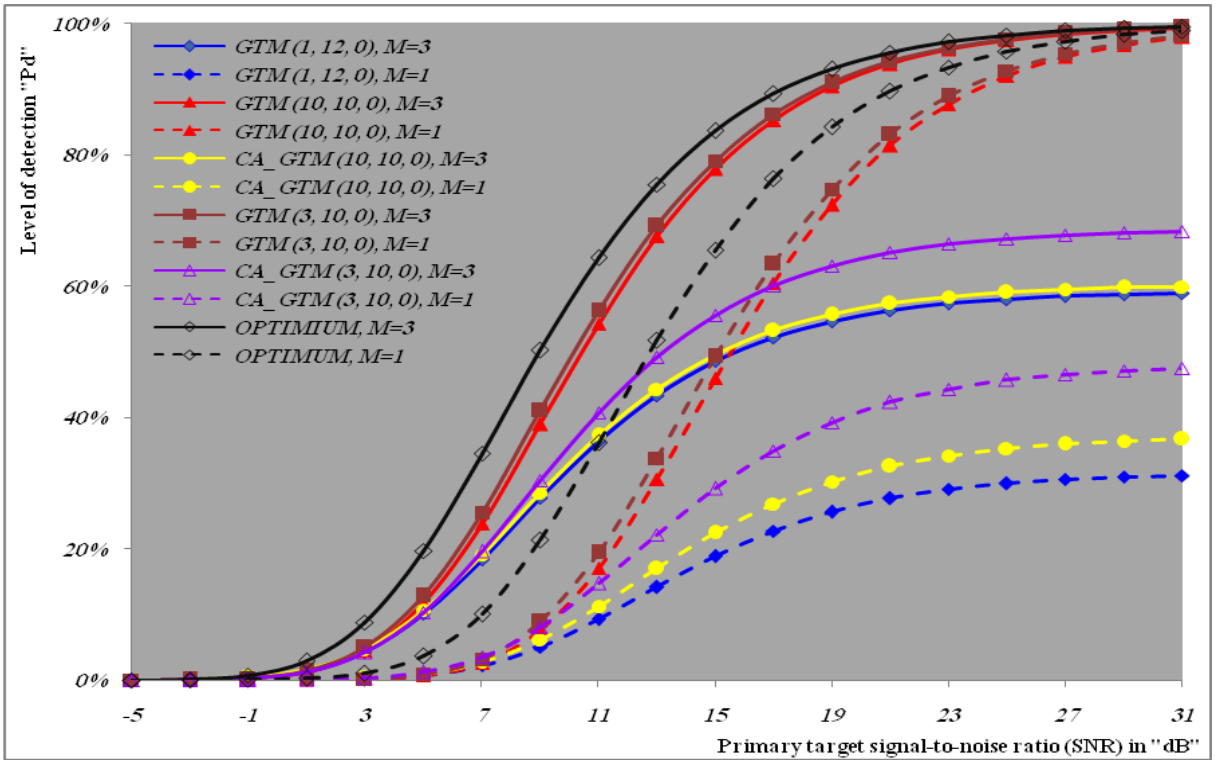

Fig.(13) Multipulse multitarget detection performance of GTM family of CFAR processors for SWI target fluctuation model when N=24, M=3, R1=R2=1, and Pfa=10-6

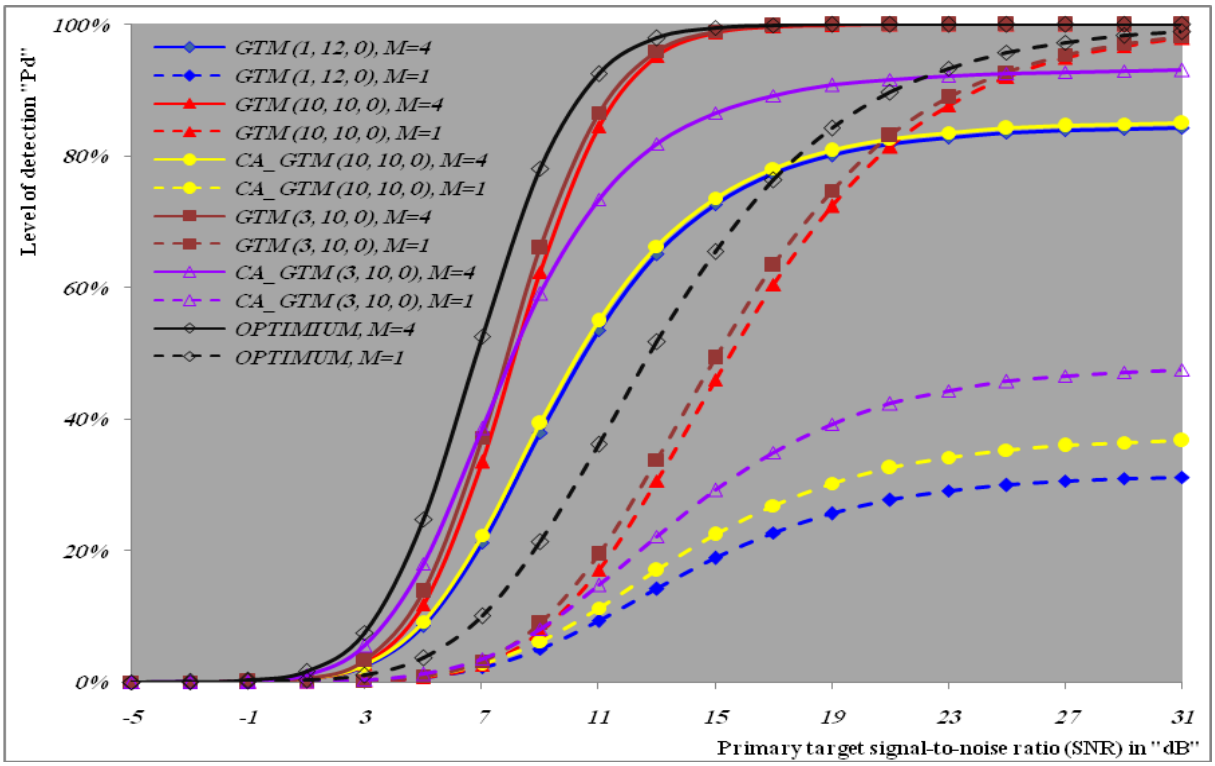

Fig.(14) Multipulse multitarget detection performance of GTM family of CFAR processors for SWII target fluctuation model when N=24, M=4, R1=R2=1, and Pfa=10-6

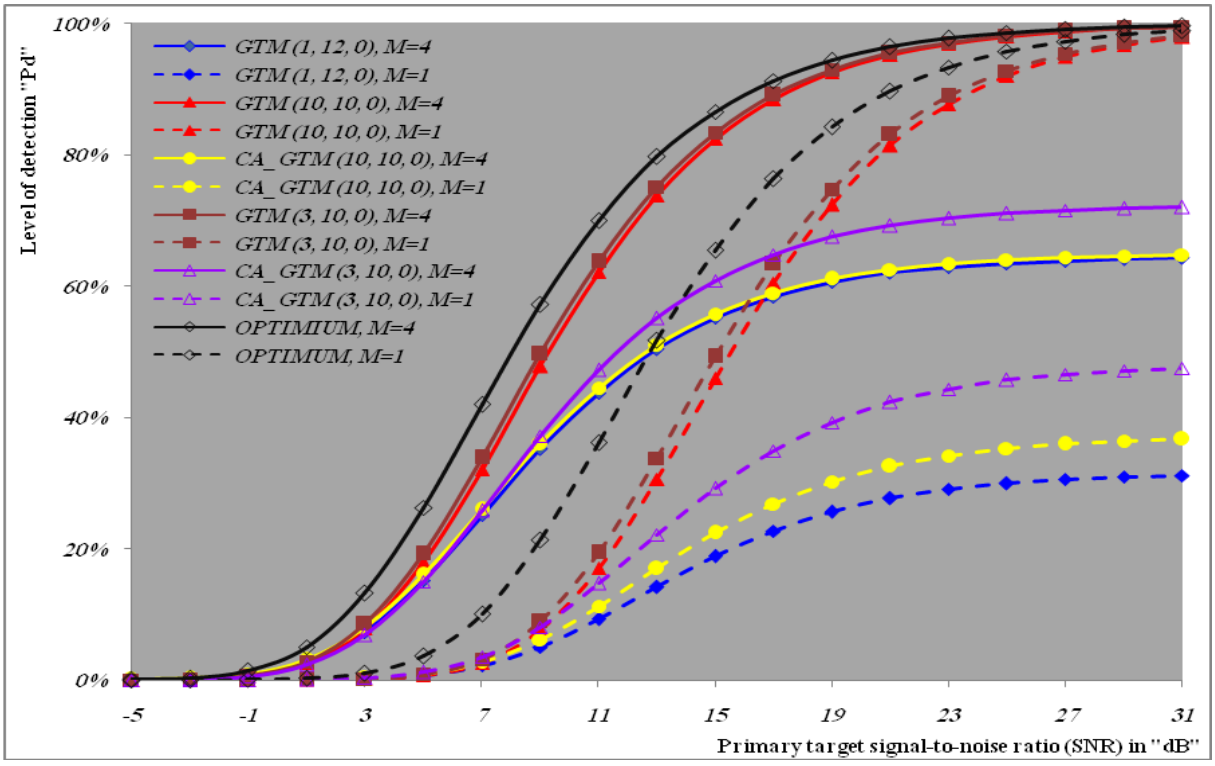

Fig.(15) Multipulse multitarget detection performance of GTM family of CFAR processors for SWI target fluctuation model when N=24, M=4, R1=R2=1, and Pfa=10-6

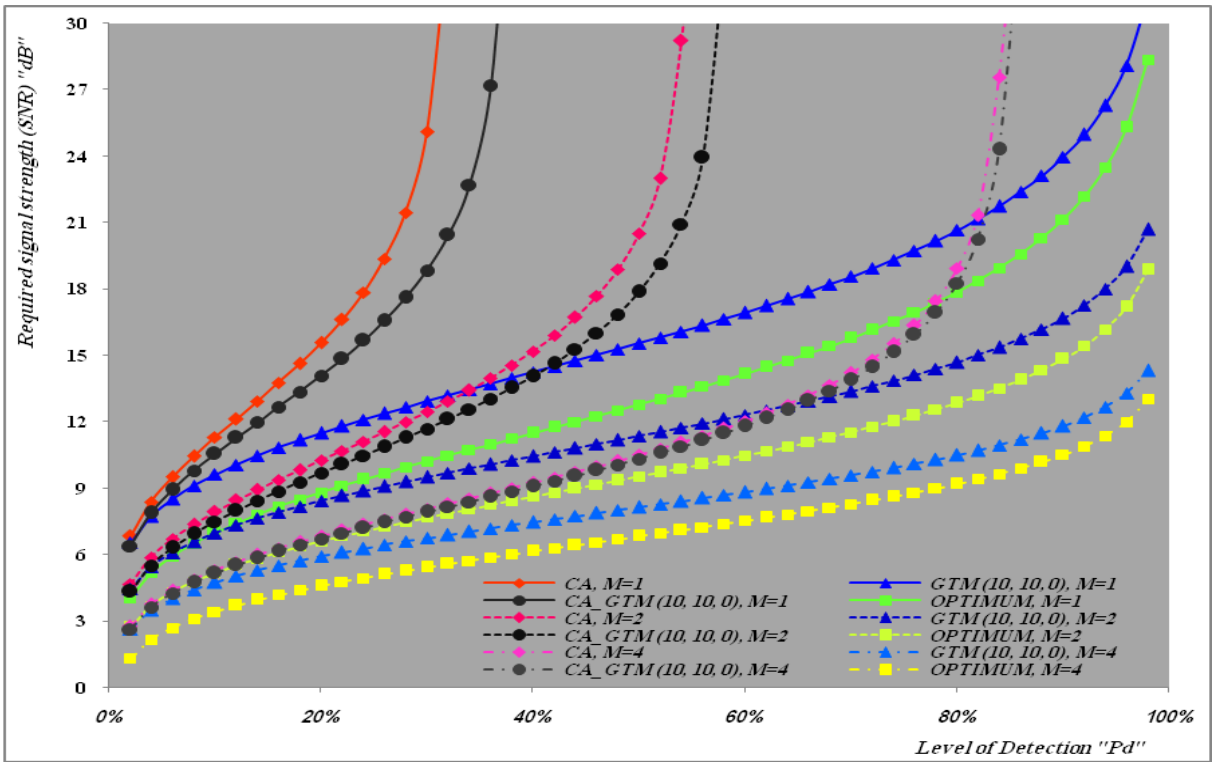

Fig.(16) Multipulse multitarget required signal strength to achieve a given level of detection of OS as well as its derived version for SWII target fluctuation model when N=24, R1=R2=1, and Pfa=10-6

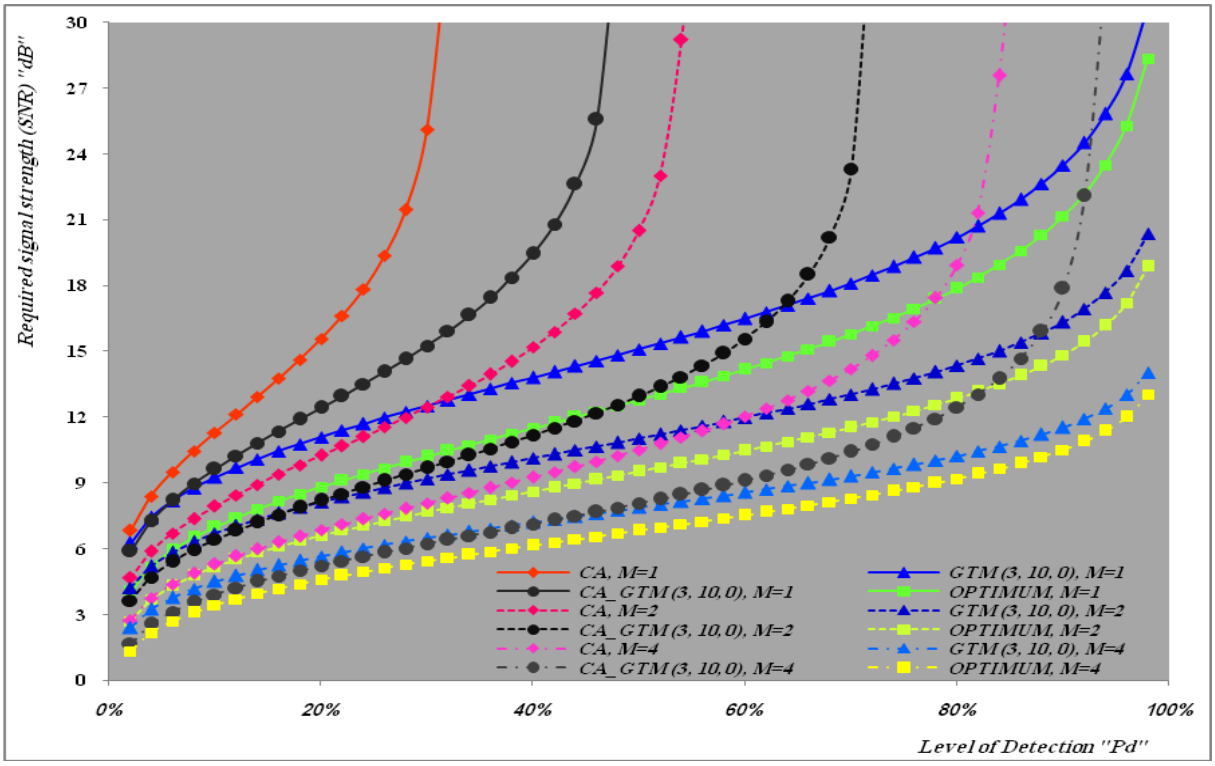

Fig.(17) Multipulse multitarget required signal strength to achieve a given level of detection of TM as well as its derived version for SWII target fluctuation model when N=24, R1=R2=1, and Pfa=10-6

References

[1] W. Q. Wang (2013), “Radar Systems: Technology, Principals and Applications”, Nova Science Publishers, Inc, 2013.

[2] El Mashade, M. B. (1994), “M-sweeps detection analysis of cell-averaging CFAR processors in multiple target situations”, IEE Radar, Sonar Navig., Vol.141, No.2, (April 1994), pp. 103-108.

[3] El Mashade, M. B. (2006), "Analysis of Cell-Averaging Based Detectors for $\chi 2$ Fluctuating Targets in Multitarget Environments", Journal of Electronics (China), Vol.23, No.6, (November 2006), pp. 853-863.

[4] El Mashade, M. B. (2008), “Performance Analysis of OS Structure of CFAR Detectors in Fluctuating Target Environments”,Progress In Electromagnetics Research C, Vol. 2, pp. 127-158, 2008

[5] Dejan Ivković, Milenko Andrić and Bojan Zrnić (2014),"False Alarm Analysis of the CATM-CFAR in Presence of Clutter Edge", Radioengineering, Vol. 23, No. 1, April 2014, pp.66-72.

[6] El Mashade, M. B. (2013), "Analytical Performance Evaluation of Adaptive Detection of Fluctuating Radar Targets", Radioelectronics and Communications Systems, 2013, Vol. 56, No. 7, pp. 321–334.

[7] Dejan Ivković, Milenko Andrić and Bojan Zrnić (2014), "A New Model of CFAR Detector", Frequenz 2014; 68(3–4): 125 – 136.

[8] El Mashade, M. B. (2015), “Adaptive Detection Enhancement of Partially-Correlated $\chi 2$ Targets in an Environment of Saturated Interference”,Recent Advances in Electrical & Electronic Engineering, Volume 8, 2015.

[9] S. W. Hong and D. S. Han (2014), "Performance Analysis of an Environmental Adaptive CFAR Detector", Hindawi Publishing Corporation Mathematical Problems in Engineering Vol. 2014, pp. 1-7.

[10] El Mashade, M. B. (2001), "Postdetection integration analysis of the excision CFAR radar target detection technique in homogeneous and nonhomogeneous environments", Signal Processing “ELSEVIER”, Vol. 81 (2001), pp.2267–2284.

[11] F. J. Jen, M. Gialich, B. Lambrecht, Z. Aliyazicioglu, H. K. Hwang (2012), "Performance Analysis of a new CFAR Algorithm under Heterogeneous Environments", Proc. of Int. Conf. on Advances in Signal Processing and Communication 2012 ACEEE, pp.107-110.

[12]El Mashade, M. B. (2013), "Postdetection Integration Analysis of Adaptive Detection of Partially-Correlated $\chi 2$ Targets in The Presence of Interferers", Majlesi Journal of Electrical Engineering, Vol. 7, No. 3, September 2013, pp. 43-58.

[13] El Mashade, M. B. (1998), "Multipulse analysis of the generalized trimmed mean CFAR detector in nonhomogeneous background environments", AEU, Vol.52, No.4, (Aug. 1998), pp. 249-260.

[14] El Mashade, M. B. (2016), "Heterogeneous Performance Evaluation of Sophisticated Versions of CFAR Detection Schemes ", Accepted for Publication in Radioelectronics and Communications Systems.